The Uppermost Nappes in the Asterousia Mountains - Coast Road Platia Permata to Lutra

View of the coastline between Geroskampos and Kali Limenes. It represents the border between the crystalline Asterousia Nappe and the "Arvi Nappe". White marble, red slate/marl and basalts are overthrust by amphibolites and gneisses. Along the coast road there are several thrust planes displaying cataclastic rock.

Compiled by George Lindemann, MSc.

Berlin, August 2024

Content

Appendix

Introduction

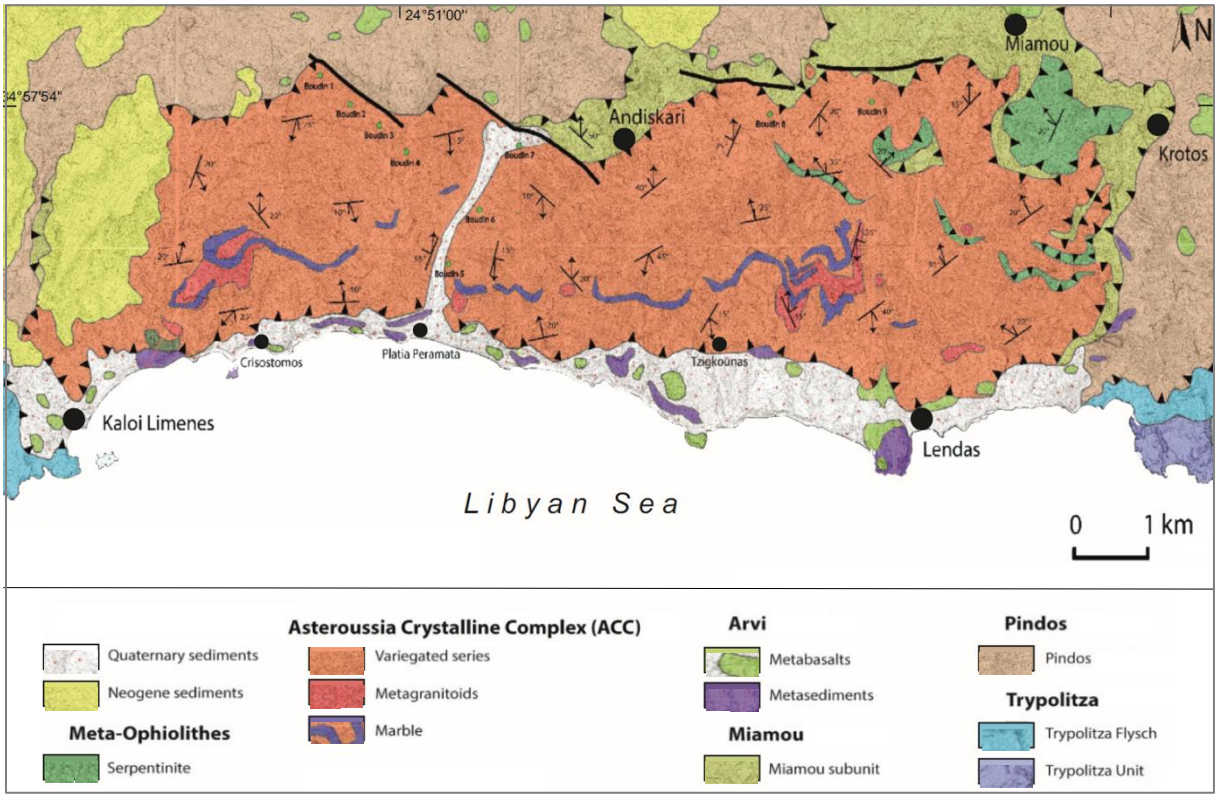

Geological map of the western part of the Asterousia Mountains showing the area between Kaloi Limenes and Lendas. Source: Zulauf G. et al., 2023, (modified after Davi and Bonneau 1972; Thorbecke 1987; Tortorici et al. 2012; Neuwirth 2018).

On Crete, the Uppermost Unit has been subdivided into several subunits differing in their lithology and in the grade and timing of metamorphism. One of the main subunits is called the Asterousia Crystalline Complex (ACC), which consists of amphibolite facies metamorphic rocks, intruded by Late Cretaceous granitoids. The ACC has been correlated with the southern margin of the Pelagonian domain of mainland Greece and therefore belongs to the Internal Hellenides (e.g. Aubouin & Dercourt, 1965; Bonneau, 1972; Martha et al. 2017). Other tectonometamorphic nappes within the Asterousia Mountains ascribed to the Uppermost Unit, but not belonging to the Pelagonian domain, include the prehnite-pumpellyite facies "Arvi" subunit, which is often interpreted as a Maastrichtian seamount at the northern margin of the Pindos Ocean (Palamakumbura, Robertson & Dixon, 2013). Another subunit belonging to the Uppermost Unit, that is well exposed south of the Dikti Mountains (Martha et al. 2017), is the Greenschist Unit that is characterized by fine-grained epidote-amphibole schist with a mid-ocean ridge basalt (MORB) -type signature (Reinecke *et al.* 1982; Martha et al. 2017). However, the Greenschist Unit has not yet been reported along the coast of western Astrousia Mountains. This field guide is concerned with the geology along the western coastline of the Astrousia Mountains (Platia Permata to Lutra) and looks particularly at the thrust plane between the ACC and the Arvi subunit. It also records the rocks encountered in the field and allocate them to their particular subunit.

In general, the Uppermost Unit tectonostratigaphically overlies the Tripoliza and Pindos nappes. The Pindos nappe is well exposed in the area around Lutra displaying conspicuous alternating red chert and pink/white limestone beds, which are regarded as deep marine facies. Investigations at the Lendas Peninsular also allocate the existing limestones, clastics and volcanic rocks there to the Pindos Unit (Stampfli, 2010). In addition near Lintas, Pindos flysch is overthrust by the ACC subunit representing a boundary to the Uppermost Unit.

South of the Dikti Mts. the Arvi subunit forming the base of the Uppermost Unit is reported to be thrust on to the Pindos Nappe (Martha et al. 2017). According to some authors the Arvi subunit represents a mélange with blocks of basaltic pillow lava and pelagic limestone in a flysch matrix (Fassoulas, 2001; Robert and Bonneau, 1982). However, a more coherent stratigraphy has been identified south of the Dikti Mts. (Palamakumbura, Martha et al. 2017). There the Arvi Unit consists of reddish pelagic limestone, terrigenous turbidites, pillow basalt and dolerite. Mineral parageneses from the pillow basalts point to prehnite-pumpellyite facies overprint (Robert & Bonneau 1982). Based on findings of planktonic foraminifera in the Arvi limestone (Tataris 1964), the deposition age has been constrained at Maastrichtian whilst basaltic volcanism is probably of the same age (Robert & Bonneau 1982). Geochemical data (X-ray fluorescence analyses) from the pillow basalts reveal ocean island basalt (OIB) spectra (Palamakumbura et al. 2013). *[Palamakumbura]*.

Within the Uppermost Unit, the Arvi subunit is overridden by the ACC nappe, a high-grade metamorphic unit that includes amphibolites, marbles, mica-schist and gneisses, as well as migmatites and small granitoid intrusions (Bonneau, 1972, 1984). The ACC underwent high temperature–low pressure metamorphism (Seidel et al., 1976, 1981). Dating shows that the last metamorphic event took place around Late Cretaceous time and the ACC had cooled before the Arvi Unit was created in latest Cretaceous time (Bonneau, 1976; Davis, 1967; Seidel et al., 1976). The high structural position of the ACC nappe suggests general affinity with the Pelagonian Zone of mainland Greece. However, the ACC may also correlate with metamorphic rocks exposed in the Aegean Cyclades or the southern Menderes Massif of western Turkey.

Scattered exposures of dismembered ophiolitic rocks in central and eastern Crete are dated at ~160 Ma (Koepke et al., 2002). These can be correlated with the Jurassic ophiolites exposed throughout the Pelagonian Zone as far south as, and including, the southern Peloponnese (I.G.M.E, 1983). The Uppermost Unit of Crete was emplaced onto the previously assembled Tripoliza and Pindos nappes during Late Eocene/Early Oligocene times in response to the closure of a Tethyan ocean to the north (Fassoulas, 1998; Hall et al., 1984; Van Hinsbergen et al., 2005a, 2005b) *[Palamakumbura]*. [1]

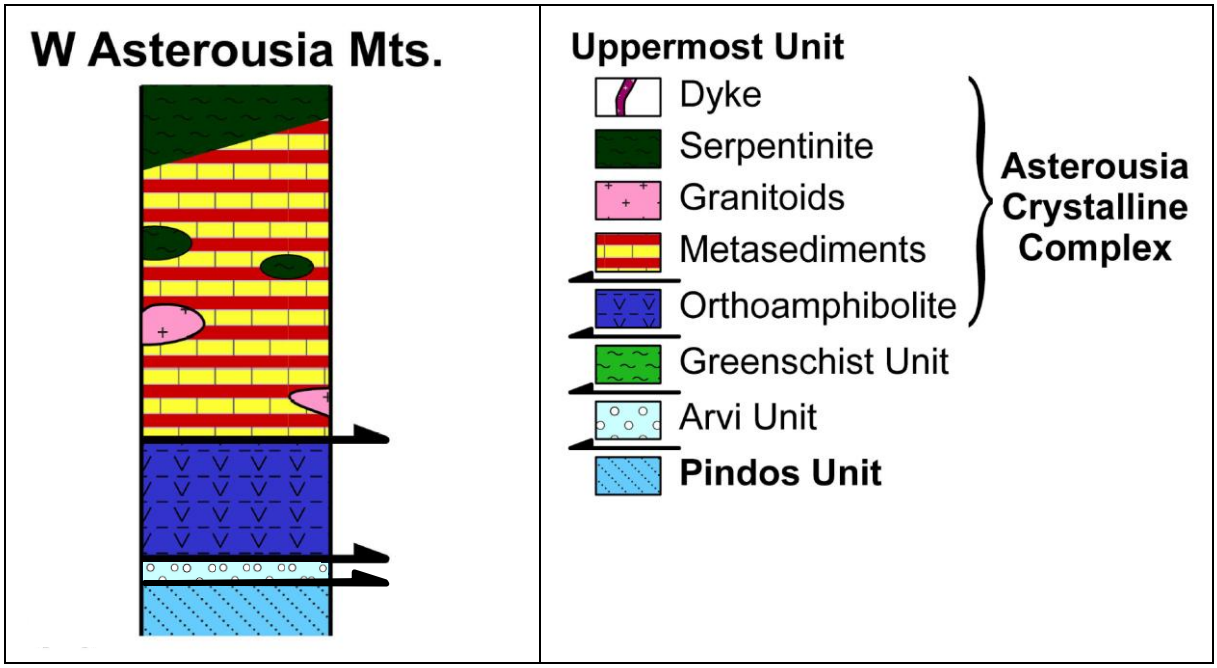

Column showing the tectonostratigaphic sequence of the Uppermost Unit in the western Asterousia Mountains (after Koepke & Seidel 1984). The column is not to scale. Slightly modified after Martha, et. al 2017

[1] See also My GeoGuide No. 22: The Uppermost Nappes in the Asterousia Mountains - Coast Road Kali Limenes to Chrysostoms.

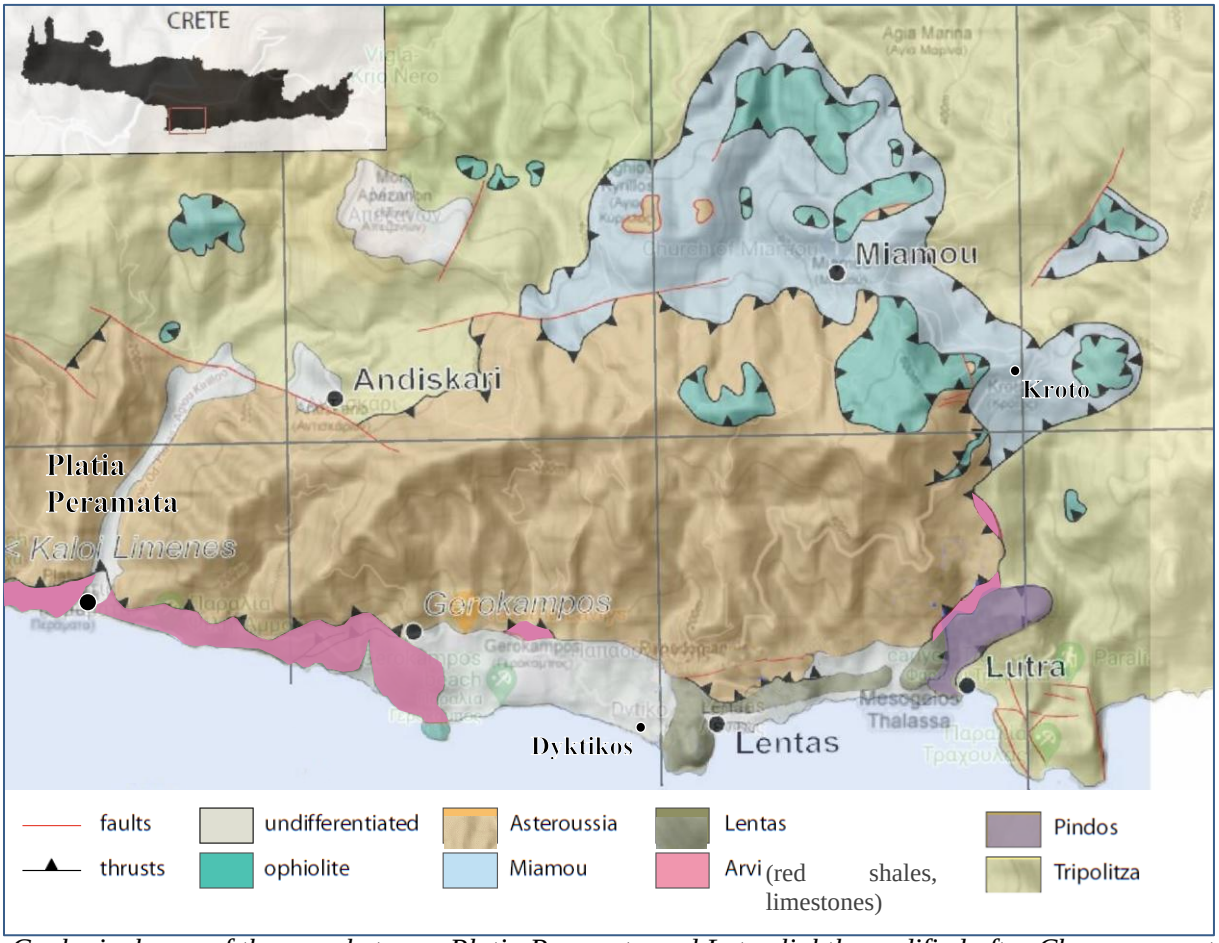

Geological map of the area between Platia Peramata and Luta slightly modified after Champ[illegible] et al., 2010 and Vachard D. et al. 2013: Tectonic map - Andiskarion sheet, modified after Davi & Bonneau (1985) [Stampfli, 2010: Field Course]

1 Platia Peramata - Dytikos Beach

Location of Outcrops I to IV [source of image Google Maps]

Outcrop I: View of the coast just west of Platia Peramata. The rock sequence is similar to the one at Sinifas Beach consisting of limestone, red slate/marl and probably volcanic rock.

1.1 Olistolith and Basalt

Outcrop II: Red slate/marl

Outcrop III: Red slate/marl

Outcrop IV: Limestone olistolith thought to belong to the Pindos Unit embedded in flysch. Detachment from its original structure, transport and emplacement is reported to be the result of gravity flow (bushes for scale).

Outcrop IV: "Pindos" limestone olistolith displaying slickensides. The slickensides indicate movement along a fault plane.

Outcrop IV: Closeup of a slickenside surface. A slickenside is a smoothly polished surface caused by frictional movement between rocks along a fault. This surface is typically striated with linear features, which indicate the direction of movement.

Outcrop IV: "Pindos" limestone olistolith containing numerous large and small calcite veins

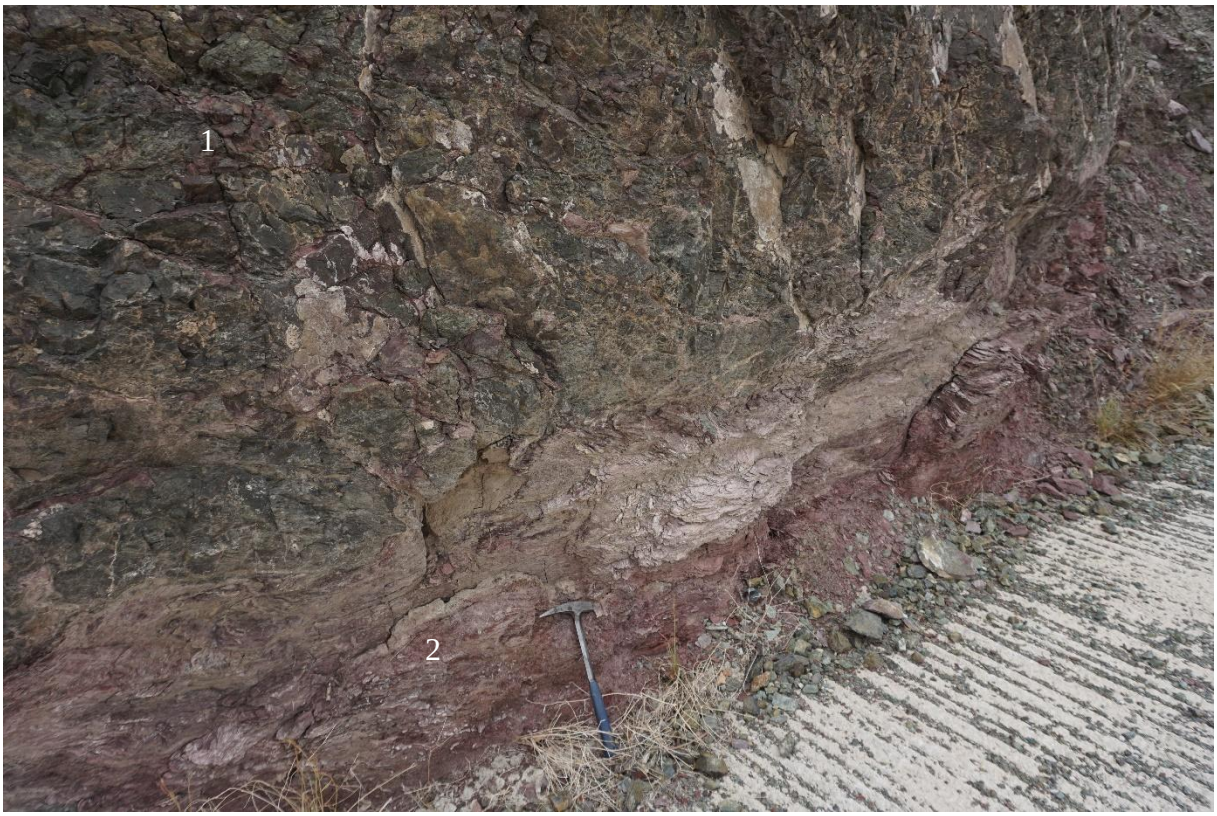

Outcrop IV, Arvi subunit: 1: metamorphically or hydrothermally altered basalt. 2: pelagic red slate/marl

Outcrop IV, Arvi subunit: Metamorphically or hydrothermally altered basalt

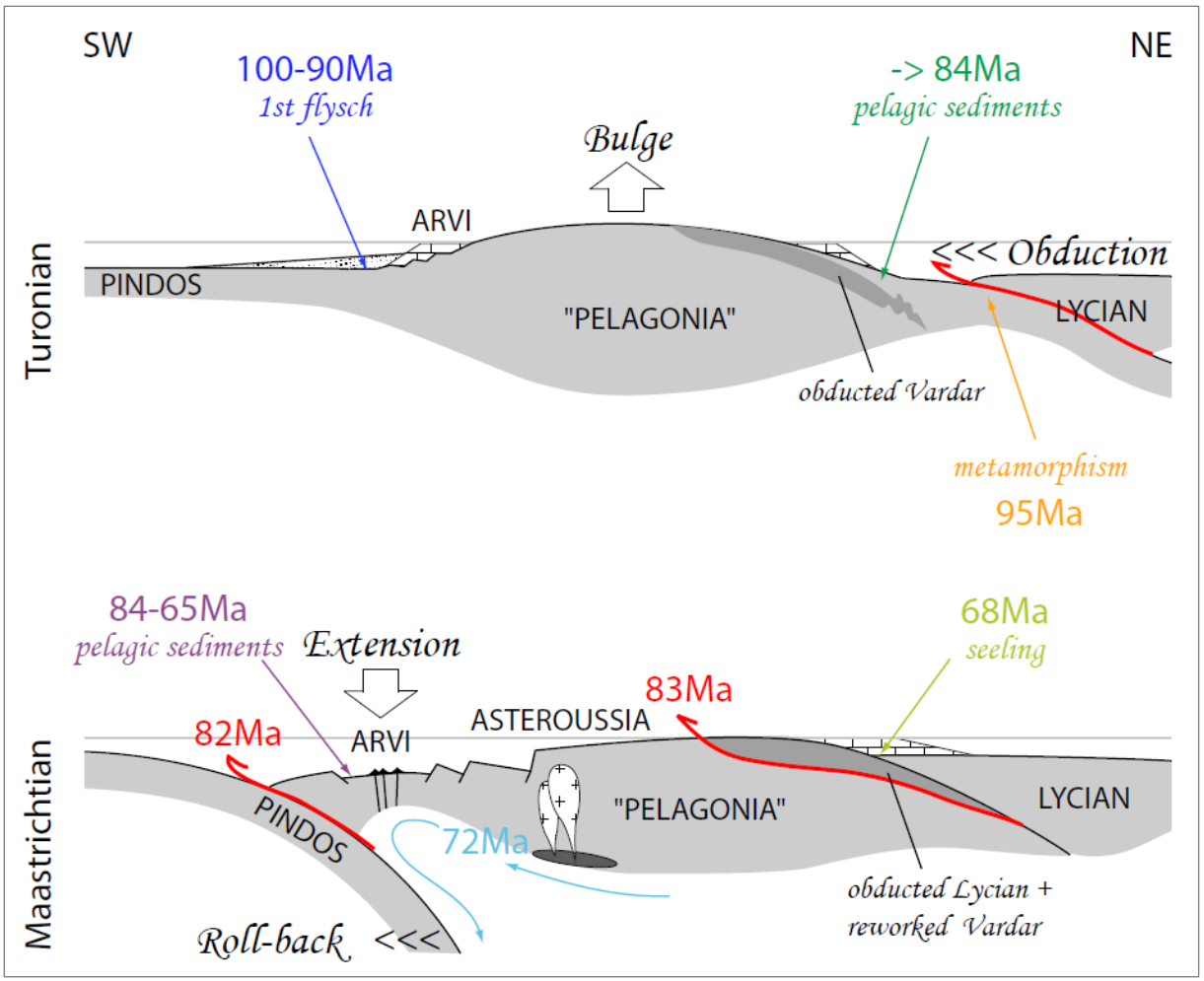

Schematic sections showing the possible position of the Arvi unit and its development during Late Cretaceous possibly as a sea mount [Stampfli, 2010].

1.2 Thrust Planes

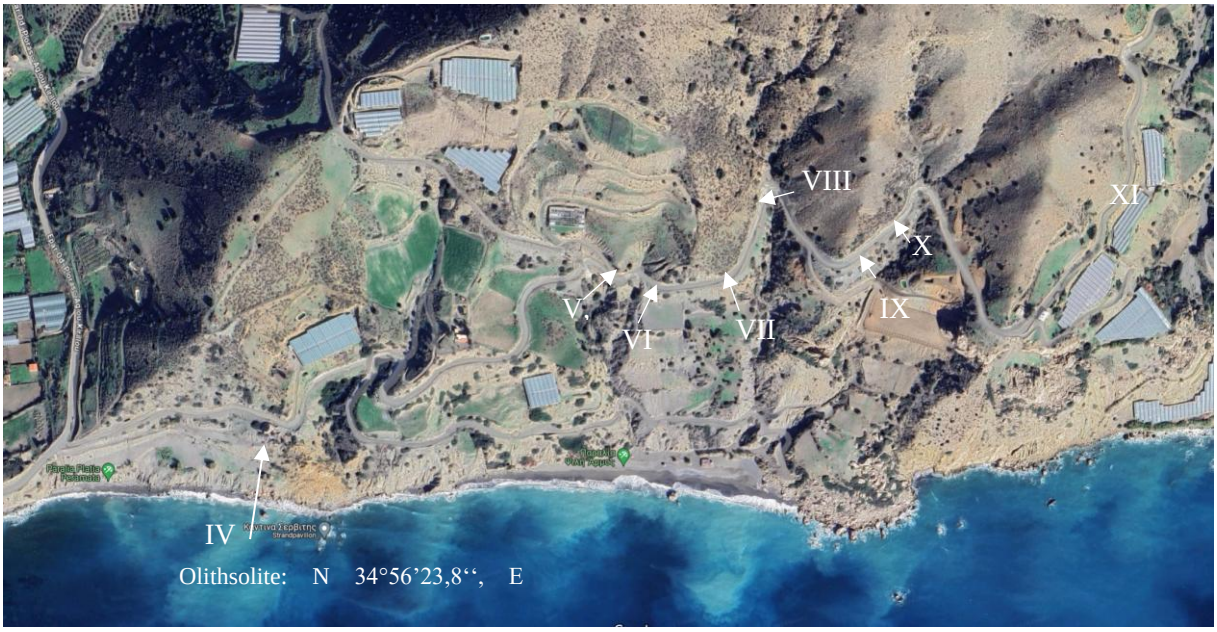

Location of Outcrops IV to XI [source of image Google Maps]

Outcrop V, ACC. a: Thrust fault within the Asterousia Crystalline Complex (ACC) displaying northward dip at contact to marble body. 1: marble lens, 2: amphibolite (metapelite).

Outcrop V, ACC. Closeup of previous picture (box). 1: marble displaying brittle deformation

Outcrop VI, ACC. Thrust fault within ACC-nappe. 1: marble body, 2: overthrust cataclastic amphibolite

Outcrop VI, ACC. Northward dipping thrust plane within the ACC-nappe. 1: marble body, 2: overthrust cataclastic amphibolite

Outcrop VI, ACC. Closeup of the thrust plane. 1: marble, 2: cataclastic amphibolite. Cataclastic texture is characteristic of brittle thrust plane deformation.

Outcrop VI, ACC. 1: marble body. 2: black chert lens could be due to radiolarites, indicating possible pelagic origin (i.e. deposited in an open ocean and/or deep water environment).

Outcrop VI, ACC. Sample from the marble body displaying light and dark grey inhomogeneous texture.

Marble sample from a thrust fault within the ACC-Nappe. Relic bedding and medium grained calcite crystals. Orange colouring is due to Fe-Oxides at fissure.

Marble sample from another thrust fault 40m further East. Creamy white with relic bedding and medium grained calcite crystals.

Outcrop VI, ACC. At some places the marble displays an interesting texture, which could be due to relic organisms such as algae, coral or sponges no longer preserved due to metamorphism. As opposed to radiolarite, reef carbonates would indicate shallow water conditions.

The paragneiss, amphibolite and calcsilicate rocks throughout most the mountain range contain small and large marble bodies, whereby the larger bodies often form the tops of the mountain ridges. Extended thin layers of marble also exist along the southern mountain sides and smaller lenses are often encountered at the contact to thrust planes. The marble is frequently well bedded although it has been metamorphically over printed. It also displays young post-metamorphic faulting vertical to the bedding that sometimes gives it a "graben and horst" character. Based only on mesoscopic assessment it is not clear whether the original limestone was formed under deep or shallow water conditions. Outcrop VI at one of the thrust faults revealed radiolarite intercalations indicating pelagic conditions. However, the same outcrop might contain former relic reef material and therefore be of shallow water facies.

Outcrop VI, ACC: Amphibolite sample from outside of the thrust fault zone.

Outcrop VII, ACC. Thrust plane, 1: highly jointed and faulted amphibolite, 2: cataclastic shear zone 3: Lens shaped bodies along the thrust plane indicate shear stress.

Outcrop VIII, ACC. "Undisturbed" stratigraphic sequence. 1: amphibolite, 2: marble with orange-coloured layers. The foliation is thought to be parallel to bedding, which dips northwards.

Outcrop VIII, ACC. Closeup of the marble.

Outcrop IX, ACC. Mafic to ultramafic rock thrust on highly sheared marble within the ACC

Outcrop IX, ACC. Close up of thrust plane and shear zone. 1: mafic to ultramafic rock, 2: cataclastic marble.

Outcrop X, ACC. Continuation of previously described thrust plane. 1: serpentinized mafic to ultramafic rock, 2: marble lens.

Outcrop X, ACC. Closeup of sample of ultramafic rock.

Outcrop X, ACC. Serpentinized mafic to ultramafic rock

Outcrop XI, ACC. Paragneiss/schist displaying a series of isoclinal folds

Outcrop XI, ACC. Paragneiss/schist within the ACC displaying crenulation cleavage consisting of two generations deformation. D_1: metamorphism and growth of mica forming foliation S_1 at right angles to D_1; D_2: folding of previous S_1 foliation. In this case D_1 and D_2 appear to be in a similar direction.

During mountain building tectonic forces seldom have the same direction/stress field for long periods of time. The rule, rather than the exception, is that the orientation of tectonic forces changes continuously, as tectonic plates drift towards new directions, and mountain chains evolve through time. As a result, a foliation which developed earlier may be overprinted by a new foliation, with a brand-new orientation, that refolds the previous structure. This second foliation is called ‘crenulation cleavage ‘.

Outcrop XI, ACC. Paragneiss displaying crenulation cleavage. In this example the S_2-foliation is not distinct but is recognizable by the wavy forms created by deformation of the original foliation.

Location of Outcrops XI to XV [source of image Google Maps]

1.3 Red Slates and Marls

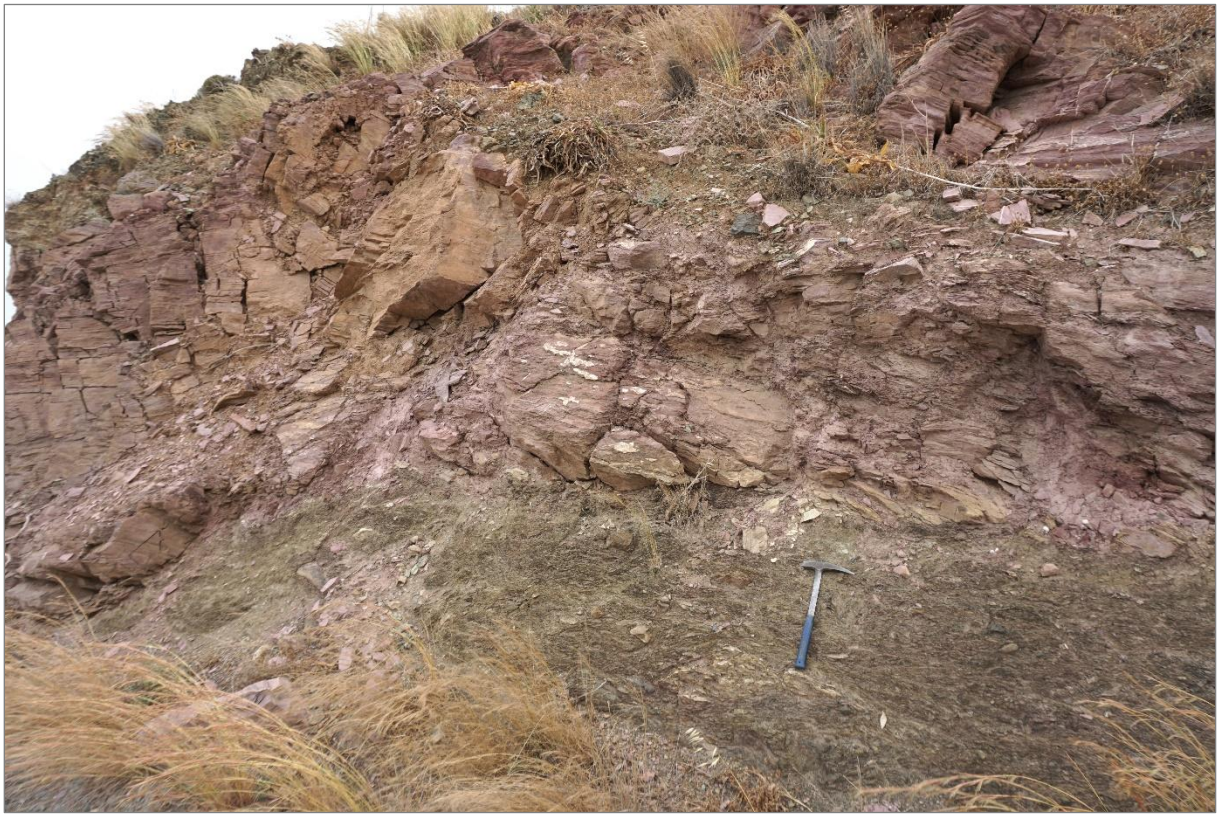

Outcrop XII, Arvi subunit. Red slate/marl thought to belong to the Arvi subunit overlying highly sheared green phyllite.

Outcrop XII, Arvi subunit. Red slate/marl reported to be associated with the Arvi-Unit. Note that it is only weakly metamorphic (prehnite-pumpellyite facies) and does not belong to the Asterousia Crystalline Complex (ACC).

1.4 Medium Grey Pelagic Limestone

One of a number of large outcrops of pelagic limestone located approx. 1km east of Platia Permata (34°56'19.3"N 24°51'57.8"E) overlain by the ACC (gneiss/schist near Outcrop XI)

Outcrop XIII. A large outcrop of limestone thought to be associated with the Arvi subunit owing to its tectonostratigaphic position and its non-metamorphic nature. Tortorici L. et al. (2011) refers on his (see geological map in Appendix) to this limestone as being pelagic.

Outcrop XIII. Sample of the limestone shown in the previous picture. Notice that the limestone has not undergone significant metamorphism (as it is not marble) and therefore cannot be part of the Asterousia crystalline nappe.

Outcrop XIII. A further sample of the limestone from a different spot nearby. It is medium grey as in the previous sample but is inhomogeneous containing dark clasts and light-coloured calcareous veins.

Along the coastline approx. one third of the rock underlying the ACC-nappe consist of medium grey coloured limestone. The limestone forms an approx. 15-30m thick layer forming cliffs at some locations. Owing to weathering it breaks up into blocks that fall into the sea. The limestone is sometimes underlain by a chaotic mixture of grey shale/slate and clastic material of different sizes. On the map by Tortorici L. et al., 2011 (see Appendix) the rocks underlying the ACC-nappe are referred to as "pelagic to oceanic sediments".

Weathered surface of a sample from the pelagic limestone beneath the ACC-Nappe. White dots are thought to be foraminifera (see arrow).

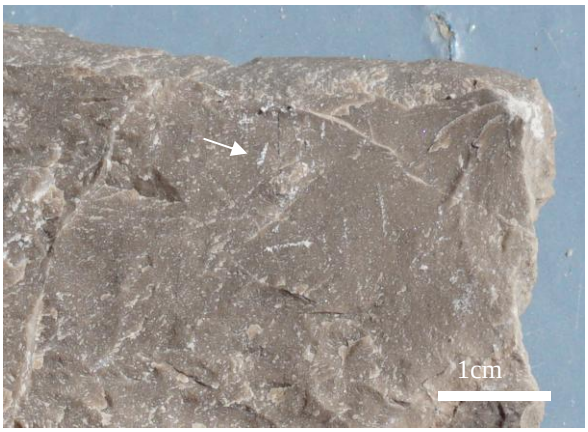

Fresh surface of the same sample from the pelagic limestone beneath the ACC-Nappe. Arrow points to possible small gastropod. The limestone is medium brownish grey.

Weathered surface of a sample from the pelagic limestone beneath the ACC-Nappe that was collected a few meters away from the sample above.

Fresh surface of the same sample from the pelagic limestone beneath the ACC-Nappe. The limestone is medium brownish grey and quite inhomogeneous with possible sparite veins.

Outcrop XIV, Arvi subunit. Phyllite

1.5 Basaltic Lava Flows

Overview of Outcrop XV, Arvi subunit. 1: paragneiss (ACC), 2: basaltic rock (Arvi subunit).

Outcrop XV, Arvi subunit. Violet and dark brown weathered basaltic rock.

Outcrop XV, Arvi subunit. Closeup of the violet and dark green weathered basaltic rock. It is thought to have undergone weak metamorphism (prehnite-pumpellyite facies) owing to its green colour indicating the presents of chlorite.

Outcrop XV, Arvi subunit. Fresh sample of basaltic rock displaying no alteration.

2 Dytikos Beach and the Lentas Hill

Location of Outcrops I to XI at Dytikos Beach, Lendas Hill and Lutra [source of image Google Maps]

Exposed along Dytikos beach and the dry river beds leading to it are marine Pleistocene sediments containing mollusc fauna of Tyrrhenian age. Conglomerates and sands dipping southwards towards the beach can be found up to 15 metres above sea level. Outcrops along the coast road near the beach are reported to contain mollusc fossils such as *Cerithium, Natica lactea, Arca noae, Glycimenis Cardium, and Lithophaga* (Boekschoten 1963) (N 34° 55.82; E 24° 54.72, N 34° 56 15 E 24° 54.47) *[Kull, 2012]*.

Dytikos beach. Pleistocene consolidated conglomerates and sands at Dytikos beach

Dytikos beach. Pleistocene conglomerate containing a bivalve shell (probably Glycimenis)

Dytikos beach. Pleistocene conglomerate. 1: some type of oyster shell.

2.1 Boulders

Examining boulders and other young sediments at the beach can reveal a great deal about the geology of a nearby mountain range. These sediments are essentially fragments of the mountain's geological history, transported by rivers and sometimes wind over time. The degree of weathering and rounding in boulders helps determine how far they have travelled from their source. Sharp, angular rocks might indicate proximity to the mountains, while smooth, well-rounded stones suggest longer transport distances. Larger boulders tend to settle closer to their source, whereas finer sediments (sand, silt, and clay) are transported further. Observing the distribution of these materials can provide clues about past river or glacial systems.

Mountain ranges undergo uplift through tectonic forces over millions of years, constantly being eroded by wind, water, and ice. The formation of sediments in principle involves uplift of mountains (for example due to the movement of tectonic plates), erosion, transportation and deposition. Ultimately, due to burial and diagenesis the sediments become sedimentary rock such as a conglomerate, sandstone or shale.

Dytikos beach. Amphibolite boulder lying on sand and beach rock

Dytikos beach. Amphibolite boulder displaying signs of anatexis.

Dytikos beach. Weathered migmatite boulder. 1: leucosome, 2: garnet,

Dytikos beach. Very hard amphibolite facies boulder displaying interesting porphyroblastic texture.

Dytikos beach. Closeup from previous picture showing fresh surface of sample. There is no apparent foliation and the porphyrobasts contain random intercalations. 1: Porphyroblast (assumption: feldspar with quarz intercalations, 2: matrix (assumption: cordierite)

2.2 The Lentas Series

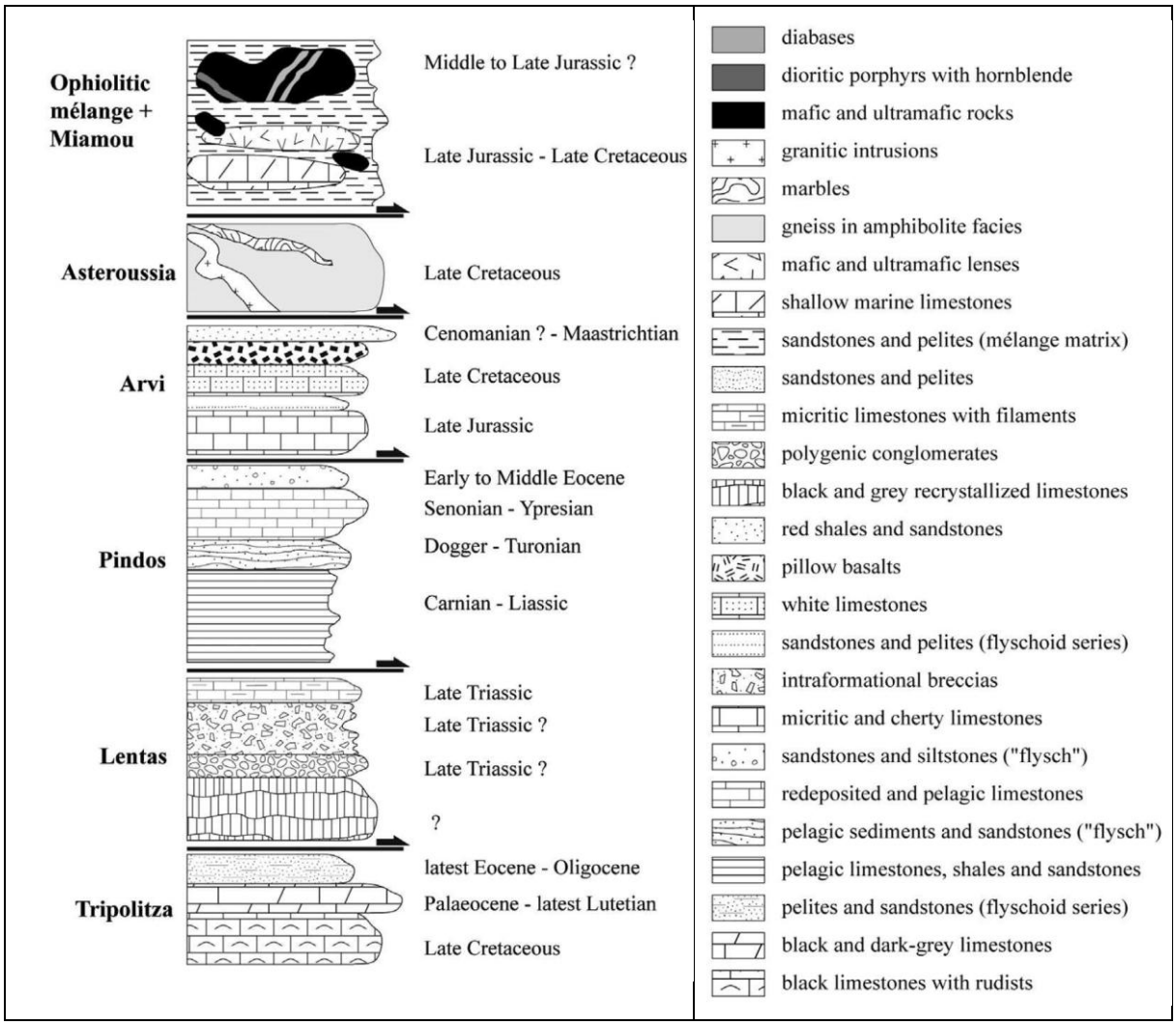

Revised tectonostratigraphic column of southern Crete showing the likely position of the Lentas Series modified from Vandelli (2010) [Vachard D. et al. 2013].

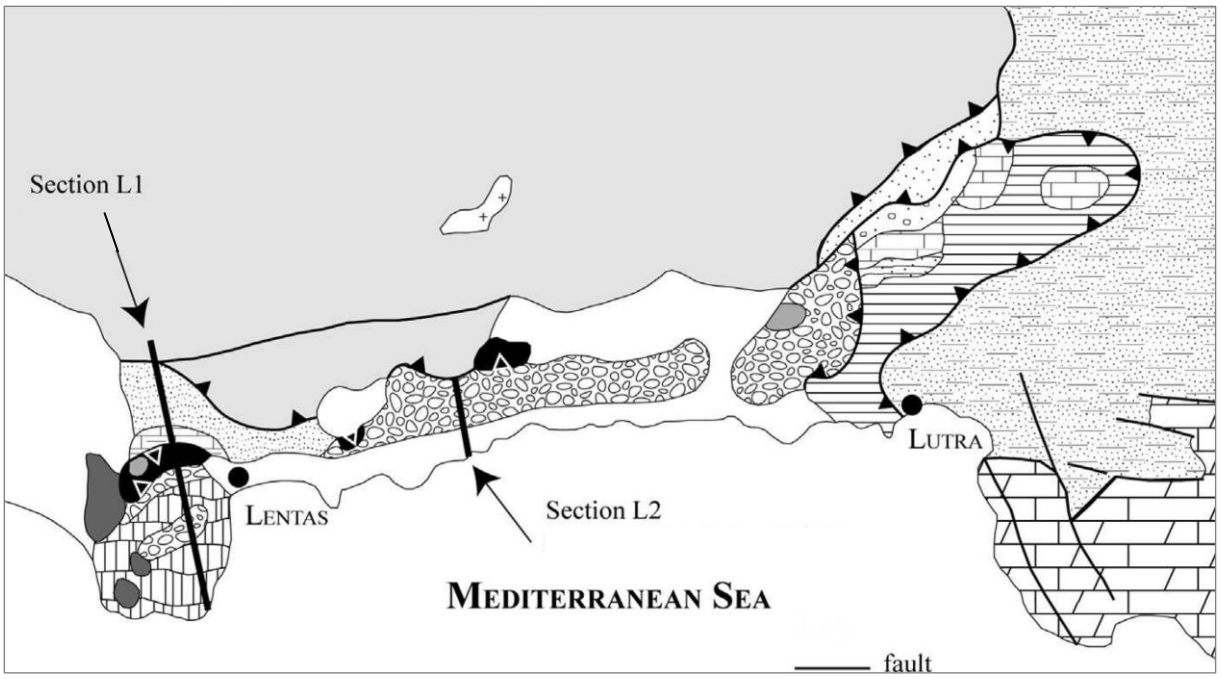

Geological map of the area between Lentas to Luta. See column for legend [Vachard D. et al. 2013].

Outcrop I. Andesite to basaltic lava. 1: Pleistocene conglomerate, 2: The lava rock is reported to belong the Lentas series, which is thought to represent the base of the Pindos unit (Stampfi, 2010).

Outcrop I. Closeup of the previous picture. Notice the light colour of the rock sample indicating intermediate composition (i.e. less mafic minerals).

Outcrop II. Lentas series, which is thought to form the base of the Pindos Unit [Stampfli, 2010]. 1: Light grey epi-metamorphic limestones and possibly younger Jurassic limestone. 2: Green conglomerate or volcanic breccia overlying the limestone.

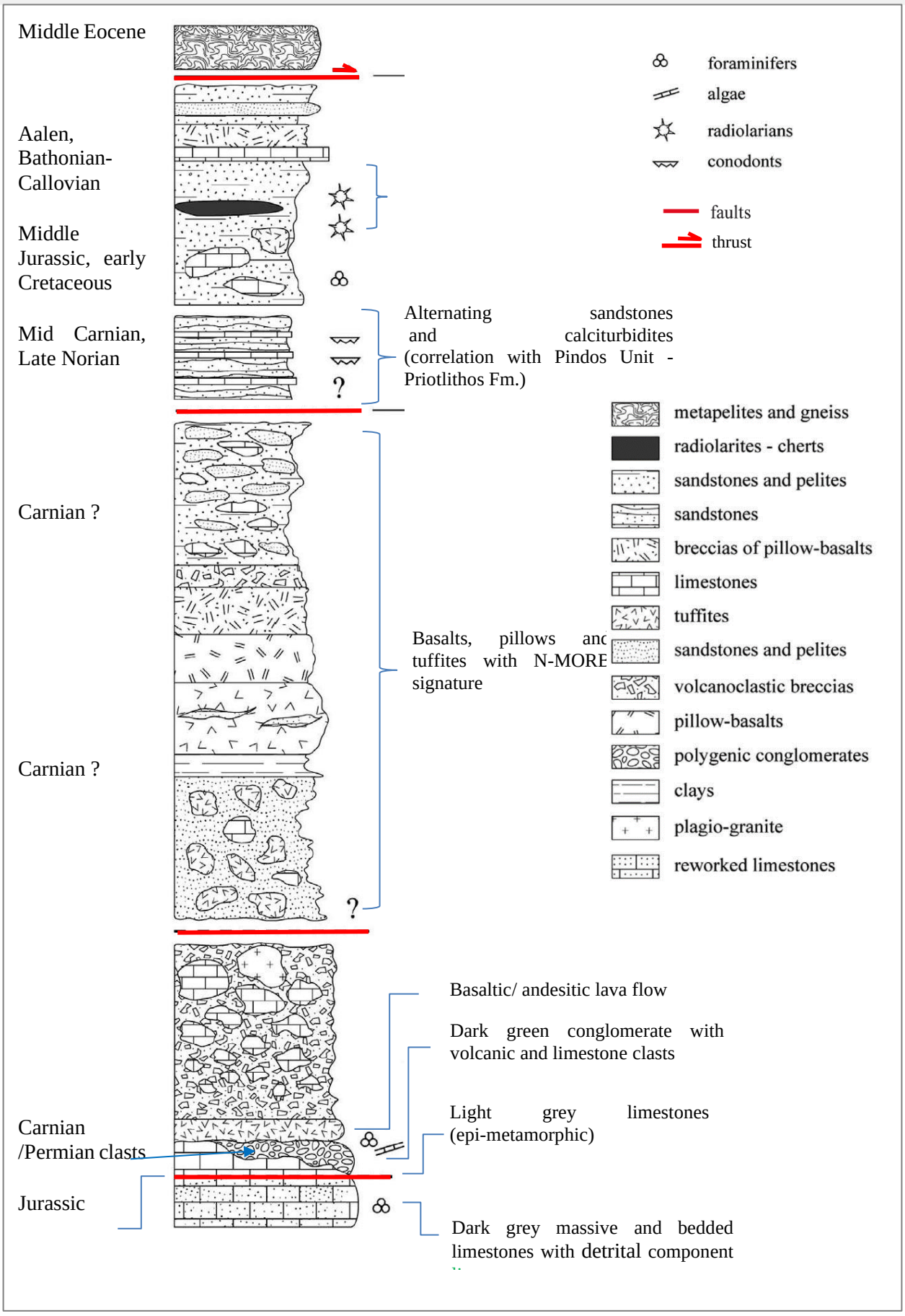

Stratigraphic column of the Lentas series (Sections L1) [Vachard D. et al. 2013]

The Lentas unit has been classically described as a Triassic sequence composed of platform carbonates, polygenic conglomerates, sandstones and limestones sequences that are ultimately overlain by a flysch of unknown age. However, some authors (Thorbecke, 1987) argue that the Lentas unit could represent an olistolith from an Upper Jurassic-Lower Cretaceous platform that was broken off and embedded within the Oligocene Pindos 2nd flysch.

Several authors (Stampfli, 2010; Vandelli, 2010; Vachard D., 2013) allocate the Lentas series to the base of the Pindos Unit, because of ages and facies similarities with equivalent series in Greece and Turkey. In particular, Vandelli, 2010 proposes that pelagic limestones alternating with sandstones and conglomerates in the Lentas sequence correspond to the Priolithos Formation of the Pindos Unit (cf. Degnan & Robertson, 1998). This is a formation belonging to the passive margin of the Pindos Ocean that is often exposed in the eastern Mediterranean; for example, the Pindos-Olonos series in the Peloponnese and in continental Greece as well as the Ethia and Mangassa series on Crete.

The Lentas series encompasses the various rocks at Lentas Hill and the lithology nearby, further east along the coast. Along the coast road the base of the Lentas series is exposed below the road. It consists of bedded limestones with a detrital component, which have been dated at Middle Jurassic-Early Cretaceous (Vandelli, 2010, Vachard D., 2013). At coast road elevation there is an approx. 50m thick layer of conglomerates containing amongst other lithologies limestone clasts of Permian (Kungurian) age. The limestone clasts have been found to contain an assemblage of fusulinids, algae and cyanobacteria indicating a shallow water environment and species of Paleotethyan affinities *[Stampfli, 2010]*.

At Lentas Hill the Middle Jurassic - Early Cretaceous limestones are prominent and are described as being more massive and a darker grey (Stampfli, 2010). This limestone is overlain by light grey epi-metamorphic recrystallized limestones that are thought to be of Carnian/Permian age and therefore must have been off-set by a fault or thrust onto the underlying darker limestones. The light grey recrystallized limestone is succeeded by a dark green and partly violet conglomerate with clasts of Middle Permian and perhaps Triassic ages (Vandelli, 2009; Vachard D., 2013) [2].

At some places basaltic/andesitic lava flows cover the conglomerate and the light grey recrystallized limestones. The basalts/andesites are fine-grained, with small feldspar phenocrystals (mostly plagioclase), and contain oxides and chlorite. The series continues with thick polygenic breccias. The volcanic matrix is dark grey with alteration from red to green. The clasts of the breccia are comparable to those from the Carnian/Permian conglomerate described above and the distinction between the two lithologies is not always possible (Vachard D., 2013). Other rocks of volcanic origin such as pillow lavas, breccias and tuffites, probably of Carnian age, follow in the succession. According to Vandelli, 2010 they have a Normal Mid-Ocean Ridge Basalt (N-MORB) signature, which is characterized by depletion in incompatible elements, meaning it has lower concentrations of elements like potassium, rubidium, and barium compared to other basalt types [3]. *[Vachard D., 2013]*

Near the top of the Lentas section, juxtaposed by recent tectonics is a series of alternating sandstones and calciturbidites, which yield late Carnian-Norian conodonts (Davi & Bonneau, 1985; Vandelli, 2010). Based on the dating of the conodonts these beds enable corelation with the Priolithos Formation with in the Pindos Unit.

[2] Note that the age of a limestone clast, determined through fossil content or radiometric dating, reflects the age of the original limestone layer from which it was eroded - not the time when the conglomerate was deposited. However, researchers sometimes use the youngest clasts within a conglomerate as a maximum age constraint for deposition. If a conglomerate contains limestone clasts of a known age, it suggests that the deposition occurred after those limestone layers were formed and eroded.

[3] see Appendix of My GeoGuide No. 24: The Uppermost Nappes of the Asterousia Mountains – Miamou to Lendas for details on partial melting and fractional crystallization).

In conclusion, Vandelli, 2010 proposes that the Lentas and Pindos units belong to the same paleogeographic realm - the Lendas series is likely to represents a volcanoclastic synrift series and the development of a passive margin of the Huğlu-Pindos Ocean. Based on the plate tectonic models of Stampfi et. al. 2009 the Pindos Ocean may be regarded as a back-arc basin of the Paleotethys.

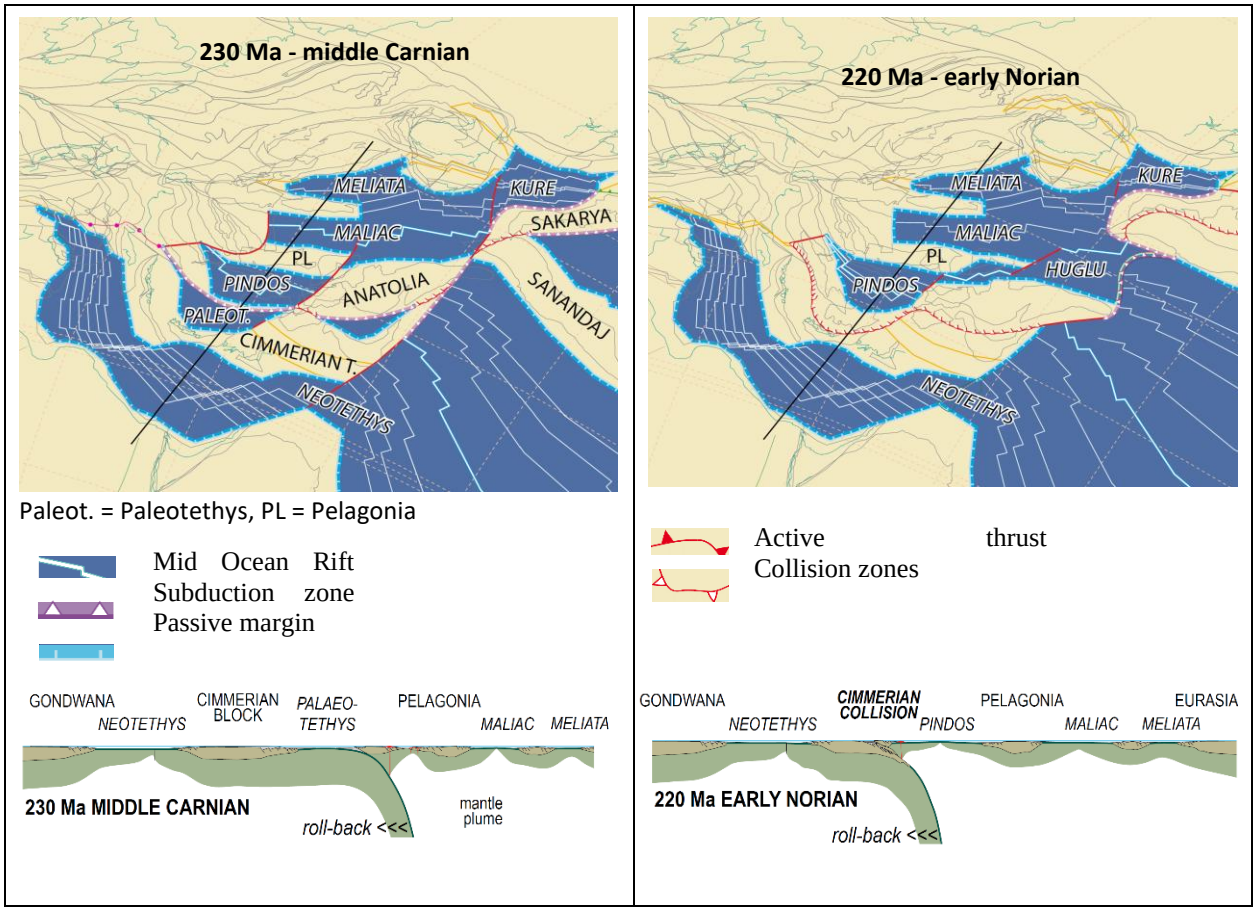

Plates tectonic models for the Upper Triassic modified after Stampfli & Hochard (2009) and Moix (2010) [Stampfli, 2010]

Outcrop II. Green conglomerate or volcanic breccia. 1: limestone clasts, 2: rounded and partly quite flat volcanic clasts. Foliation appears to dip southwards.

Outcrop II. Green conglomerate or volcanic breccia containing different clasts but mainly rounded volcanic rocks.

Outcrop II. Green conglomerate. The clasts have been deformed and are almost flat at some places. In addition, a later phase of deformation is indicated by numerous veins that cross cut the clasts.

Outcrop III. Mafic to ultra-mafic body located east of Lentas Hill

3 Lentas to Lutra (Yacht Harbour)

3.1 Pindos Unit within the Gorge

Location of outcrops IV to XI at Lutra [source of image Google Maps]

View of the gorge near Lutra looking northwards (from N 34° 56,12; E 24° 56,98). The Pindos Unit forms a sequence of grey/red limestones and chert alternating with red shale. In this case they rim either side of valley. In the background the gorge narrows exposing massive grey turbidite limestones.

The Pindos domain of Greece was a deep-marine basin located between the Gavrovo-Tripolitza (Greater Apulia) and the Pelagonian units. In the Peloponnese, the Pindos-Olonos zone exposes a continuous sedimentary sequence of pelagic facies from the Late Triassic to the Paleocene, overlain by a Paleocene-Oligocene flysch. Other remnants of the Pindos Ocean, known as the Ethia-Pindos and Mangassa series, are well documented in Crete *[Vandelli A. (2010]*. The Ethia-Pindos is particularly found around the village Ethia in the eastern Asterousia Mountains. The general lithology of the Ethia-Pindos is similar to the mainland Pindos Olonos Unit but is in contrast thinner and more tectonically disrupted. Some sequences in particular the flyschoid ones are often thinner or missing.

Approximately 2km east of Lentas near Lutra, there is a Pindos sequence that is indicated to belong to the Drimos Formation (Vachard D., 2013). Based on the existing foraminifera the exposed sequence ranges from the Norian to the Paleocene/Eocene (Vachard D., 2013). The lithology at this location frequently displays the typical red and pink alternating sequences of cherts, limestone and silts indicative of a deep marine basin, but also displays turbidite beds, which is a feature of deep-sea fans or turbiditic slope aprons. The turbidites can be interpreted as orogenic flysch deposited during or after the onset of tectonic activity and could represent a transition from passive to active margin sedimentation i.e. foreland basin sedimentation at a subduction zone.

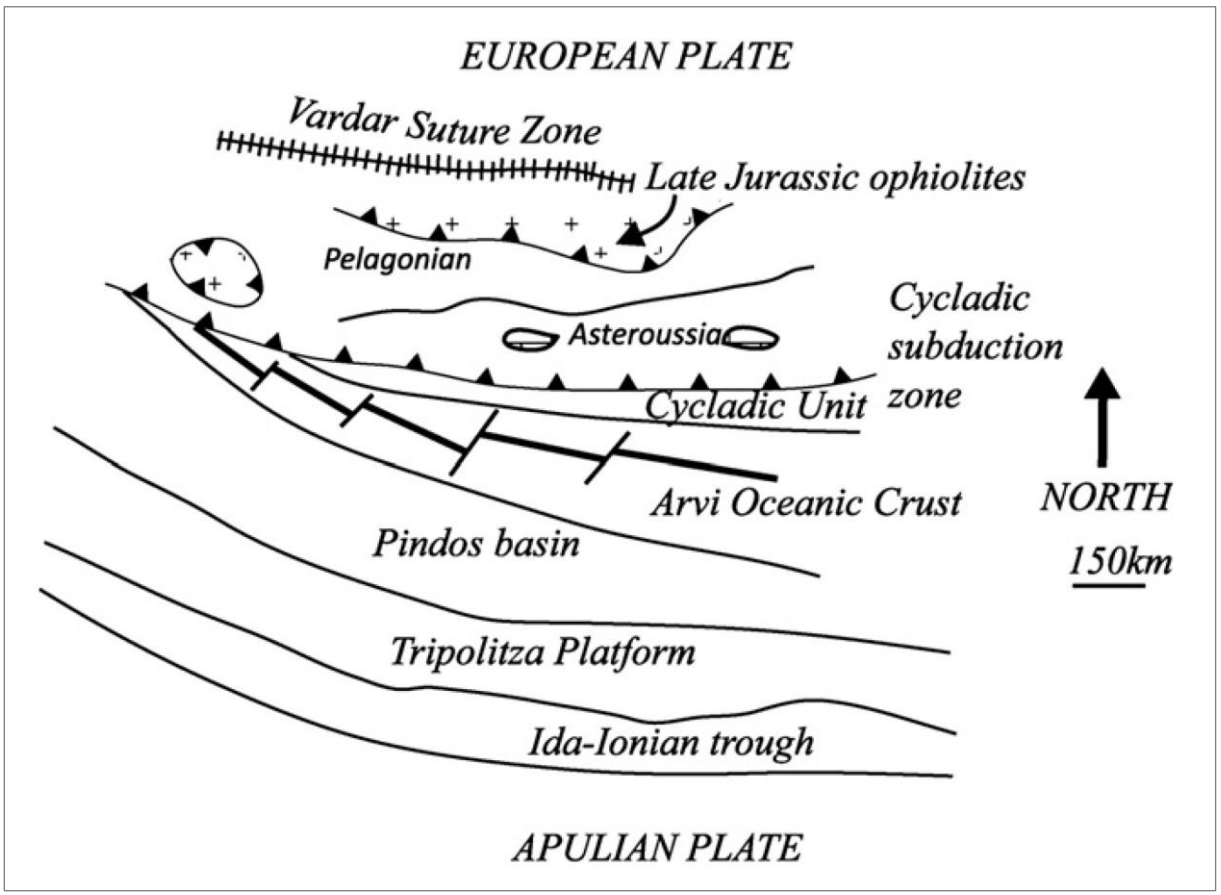

Reconstruction of the Pindos Ocean in the southern Aegean during the Late Cretaceous. Note the inferred location of the Arvi Unit (redrawn from Bonneau, 1984). [Palamakumbura R. 2012,]. The rocks of the Pindos unit represent the accreted distal parts of the northern continental margin of the Adria/Apulian microcontinent, and comprise largely deep-water Mesozoic to early Tertiary carbonates and cherts. The Tripolitza unit contains rocks of similar age that were accreted from the more proximal shallow-water platform carbonates of the colliding Adria/Apulian microplate. From Palaeocene to Eocene time onwards, both the Pindos and Tripolitza units are dominated by terrigenous flysch deposits derived from the overriding Eurasian Plate (Hall et al. 1984). [Thomson S. N.et al., 1999]

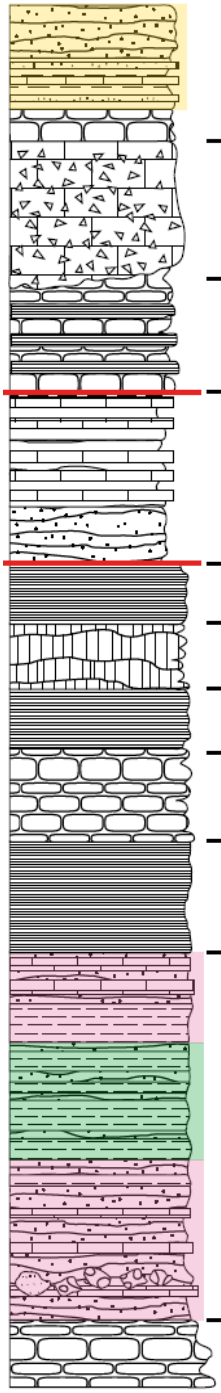

Cherty limestones interstratified with calciturbidites transcending upwards into sandstones and shales. The matrix of a mélange is thought to correspond with the Pindos second flysch.

Outcrop VIII: Mega-turbidite breccia beds with carbonate matrix and clasts of heterogenous composition and size (mm to dm). Campanian-Maastrichtian foraminifers probably reworked during the Palaeocene-Eocene.

Outcrop VII: Pink cherty limestones. Pelagic conditions

Sedimentation becomes more siliciclastic with the deposition of red shales and dark green sandstones and mudstones intercalations (Pindos first flysch?).

Red well bedded radiolarites

Green-violet well bedded radiolarites and creamy cherty limestones

Nodular limestones and calciturbidites

Outcrop VI: Pink-green radiolarites interstratified with siliceous limestones and rare calciturbidites. Pelagic conditions

Outcrop V: Alternations of pink shales, siltstones and calciturbidites with rare sandstones characterize a detrital hemi-pelagic sedimentation.

In addition, occasional polygenetic conglomeratic beds associated with channel sandstones lenses. Clasts of limestones, sandstones and mafic rocks. The matrix is red-greenish and suggests partly a volcanic origin.

Outcrop IV: Pink to grey cherty limestones alternating with light grey calciturbidites.

Composite section showing the stratigraphy of the Pindos series in southern Crete. Dating is based on foraminifers and conodonts. Due to dating and lithology the pelagic limestones appear to be equivalent to the Drimos Formation [Stampfli, 2010, Vachard D., 2013].

Outcrop IV. Pindos unit exposed at road cutting. Alternating limestone and red silty beds at road cutting

Outcrop IV. Closeup of a sample of pink coloured limestone from the sequence shown above.

Outcrop IV. Closeup of red and green silty interlayers.

Outcrop V. Pindos unit: shale and limestone sequence within dry river bed; 1: limestone, 2: red silty shale

Outcrop V. Close up of sample from a limestone bed. 1: limestone, 2: in the background red silty shale

Outcrop V. Pindos unit: alternating limestone-shale sequence within dry river bed

Outcrop VI. Pindos unit: silicious limestone beds

Outcrop VII. 1: Pink limestone, 2: red radiolarite layer

Outcrop VII. View of the base of the cliff within the gorge. Pink limestone with occasional layers of red radiolarite and are overlain by light grey massive turbidite limestone. The massive limestone contains numerous clasts of different composition (see Outcrop VIII). The boarder to the massive turbidite limestone appears to be an unconformity.

Outcrop VII. Closeup of previous picture. An unconformity in geology is an erosional or non-

depositional surface that separates two rock layers of different ages, indicating a gap in the geological record where sediment deposition was not continuous. This means that older rock layers were exposed to erosion before newer layers were deposited on top.

Outcrop VIII. Pindos unit: Boulder of light grey massive limestone displaying turbidite grains.

Outcrop VIII. Closeup of previous picture. The sample contains numerous small grains in a calcareous matrix indicating possible turbidite origin.

Outcrop VIII. Mega-turbidite of the Pindos unit. Talus from the gorge cliff face. The limestone breccia contains large clasts of different origin. There are also numerous fine grains embedded in the calcareous matix. This may have been part of a gravity flow travelling down the continental slope coming ultimately to rest in deep marine environment.

Northwards behind the cliff at the end of the gorge, basalts and red slates are thrust between the Pindos and the Asterousia nappes (see geological map). The basalts that are considered by Vachard D. et al, 2013 to belong to the Arvi subunit have a N-MORB geochemical signature. Sampfli, 2010 considers these rocks as slices of the Pindos floor. [4]

[4] See My GeoGuide - Appendix in No. 24: The Uppermost Nappes of the Asterousia Mountains – Miamou to Lentas.

4 Lutra Yacht Harbour

4.1 Strike-slip Fault

Outcrop IX. Strike-slip fault displaying well developed slickensides. The slicken lines are slightly diagonal 1: Tripoliza limestone, 2: Tripoliza flysch (Stampfli 2010, Vachard D. et al. 2013)

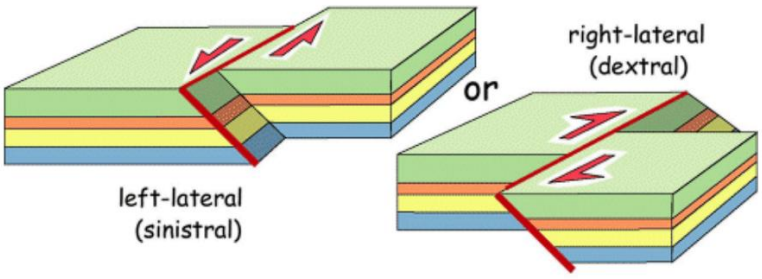

Strike-slip faults are faults where the relative displacement is parallel to the strike of the fault. [University of Leeds] Faults - fault classes

Outcrop IX: Closeup of previous picture showing fault plane of strike-slip fault

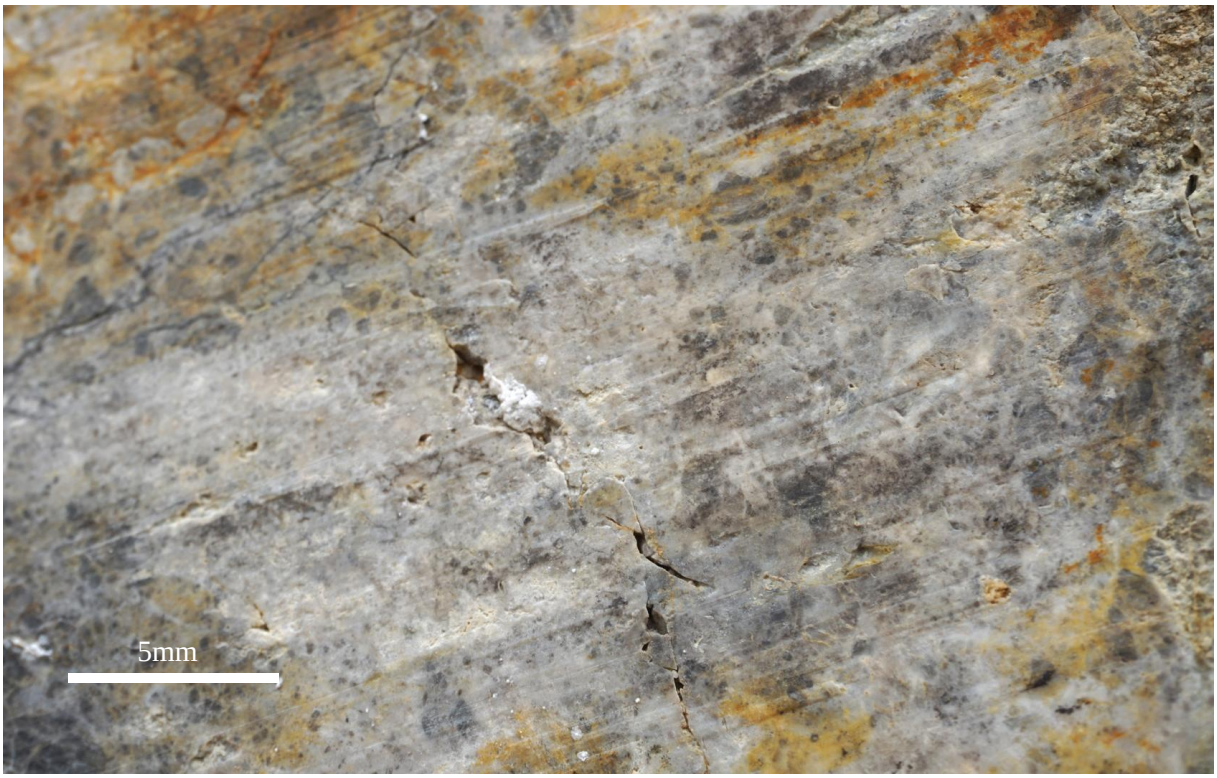

Outcrop IX. Closeup of slicken-side surface showing smooth surface and slicken lines. The surface is hard and "polished" and consists of a very fine breccia.

Slickensides are a smoothly polished surface caused by frictional movement between rocks along a fault. This surface is typically striated with linear features, called slicken lines, in the direction of movement. A slickenside can occur as a single surface at a fault between two hard surfaces. Alternatively, the gouge between the fault surfaces may contain many anastomosing slip surfaces that host slickensides.

Slickensides can be used to determine the direction of movement along the fault. They are parallel to the direction of fault motion and serve as a kinematic indicator. *[Wikiwand]*

4.2 Pindos Flysch

4.2.1 Flysch as Synorogenic Sediment

Flysch deposition is a process that is associated with mountain-building events and is therefore referred to as being synorogenic. It primarily occurs in deep-marine environments near convergent plate margins, often within foreland basins or accretionary wedges.

When orogenic belts are uplifted, erosion of mountains generates massive amounts of sediment. These sediments ranging from fine-grained shales to coarse sandstones and conglomerates are transported by rivers to the ocean basin. Gravity-driven processes, such as turbidity currents, carry the material down deep-marine slopes.

Flysch formations are largely composed of turbidites, which are layered sequences formed by underwater landslides or density-driven sediment flows. Currents sort material into distinct layers such as **c**oarse sediments (sandstones & conglomerates), which settle first due to their weight, and fine-grained sediments (shales, siltstones) that settle later. Interlayers may also represent the background sedimentation of the deep marine environment. Flysch deposits accumulate in cycles, reflecting changes in tectonic activity and sediment supply. As mountain-building progresses, the flysch basin deepens, accommodating more sediment. Over time, increasing tectonic compression leads to nappe stacking**,** incorporating flysch into deformed rock sequences.

4.2.2 First and Second Pindos Flysch

The First Flysch and Second Flysch within the Pindos Unit represent distinct sedimentary sequences that formed during different geological periods. At the beginning of the Upper Cretaceous (Cenomanian), the existing pelagic shale-chert-limestone sequences were replaced by a more clastic sedimentation consisting of sandstones, shales, and turbidites reflecting an active tectonic environment with significant sediment influx. In central Crete these deposits called “First Flysch” or “Cretaceous Flysch” (Bonneau & Fleury, 197l) consisted mainly of limestone breccias and marls. During the Turonian the First Flysch was replaced by fine-grained, platy pelagic limestones and detrital limestones with occasional chert nodules reflecting quieter tectonic conditions *[Kull]*.

The Second Flysch is a much younger sequence of turbidites that was deposited during the Eocene to Oligocene period during increased tectonic activity and uplift. It often contains coarser sediments**,** including conglomerates and sandstones, indicating the shift in depositional conditions.

Outcrop X. View of the flysch sequence at the Yacht Habour displaying folds at the upperpart of the outcrop and a relatively undisturbed but faulted flysch sequence at the lower part. [5]

Outcrop X. Lower part of the flysch sequence with fault planes is in two different directions.

[5] *Stampfli 2010, and Vachard D. et al. 2013 regard the flysch to be associated with the Tripoliza Unit. However, other authors consider it to be Pindos flysch.*

Outcrop X. Turbidite bed displaying duplex structures resulting from compressional stress parallel to bedding plane. The single bed appears to have compensated for shortening by forming duplex structures along a fault or thrust plane. 1: duplex structures or kink band, 2: compression compensated for by folding (N34°55‘59‘‘, E024°57‘13‘‘).

Outcrop X. Silty limestone from kink band indicating graded bedding and deposition by turbidity flow

Outcrop X: Several small thrust planes indicating that the flysch beds were push on top of each other like a pack of cards.

Outcrop X. Graded bedding sequence indicating fining upwards. A typical feature of turbidites and flysch deposits.

Outcrop XI, Flysch at the beach next to the habour. 1: folded sequence of silty shale and limestone (rucksack for scale). 2: large limestone blocks containing white veins at right angles to bedding plane.

Outcrop XI: Closeup of sample from the thin limestone beds. Fine sandy/silty limestone or calclutite

5 References

Alexandra van der Geer1 & George Lyras, 2011: Field Trip Guidebook European Association of Vertebrate Palaeontologists, 9th Annual Meeting Heraklion, Crete, Greece 14-19 June, 2011

Alves, T. Cupkovic T., 2018: Footwall degradation styles and associated sedimentary facies distribution in SE Crete: Insights into tilt-block extensional basins on continental margins; School of Earth and Ocean Sciences, Cardiff University, United Kingdom; Husky Energy, Atlantic Region, St. John's, Canada

Brack P., Meister P. H., Bernasconi S., 2013: Dolomite formation in the shallow seas of the Alpine Triassic, Article in Sedimentology · Feb. 2013, DOI: 10.1111/sed.12001]

Brandes C. et al., 2014: Fault-related folding: A review of kinematic models and their application, Institute for Geology, Leibniz Universität Hannover, Callinstr. 30, 30167 Hannover, Germany

Champod E. et al., 2010: Stampfli Field Course: Tectonostratigraphy and Plate Tectonics of Crete, Université de Lausanne, September 2010

Chatzaras, v., Xypolias, P. & Doutsos, T (2006): Exhumation of high-pressure rocks under continuous compression: a working hypothesis for the southern Hellenides (central Crete. Greece). - Geol. Mag. 143: 859-R76.

Cowan (1985), Gesteine bestimmen, Teil 2: Minerale https://www.kristallin.de/gesteine/index.htm

Fassoulas C., 2000: The tectonic development of a Neogene basin at the leading edge of the active European margin: the Heraklion basin, Crete, Greece, Natural History Museum of Crete, University of Crete, Heraklion 71409, Greece

Fassoulas C., Rahl J.M., 2004: Patterns and Conditions of Deformation in the Plattenkalk Nappe, Crete, Greece: A Preliminary Study, Natural History Museum of Crete, Yale University, New Haven, Connecticut

Granger D.E., 2007: Cosmogenic Nuclide Dating - Landscape Evolution, in Encyclopedia of Quaternary Science, Pages 445-452

Kull U., 2012: Kreta, Sammlung geologischer Führer

Lacinska A. M. et. al., 2016: Mineralogical characterisation of serpentine minerals in the context of carbon capture and storage by mineralization. Preliminary results, British Geological Survey, Environmental Science Centre, Nicker Hill, Keyworth, Nottingham NG12 5GG, United Kingdom

Langosch A. et al, 2000: Intrusive rocks in the ophiolitic melange of Crete ± Witnesses to a
Late Cretaceous thermal event of enigmatic geological position, Institut für Mineralogie und Geochemie, Universität zu Köln.

Martha S. et. al., 2018: The tectonometamorphic evolution of the Uppermost Unit south of the Dikti Mountains, Crete

McClay K.R.: Glossary of thrust tectonics terms, Department of Geology, Royal Holloway and Bedford New College, University of London, Egham, Surrey, England

Miller W., 1977: Geologie des Gebites Nördlich des Plakias-Bucht, Kreta, Freiburg im Breisgau, Diplomarbeit

Mountrakis D., Kilias A., Pavlaki A., Fassoulas C., Thomaidou E., Papazachos C., Papaioannou C., Roumelioti Z., et al., 2012: Neotectonic study of Western Crete and implications for seismic hazard assessment, Journal of the Virtual Explorer, Electronic Edition, ISSN 1441-8142, volume 42, paper 2 In: (Eds.) Emmanuel Skourtsos and Gordon S. Lister, The Geology of Greece, 2012.

Ogata K. et. al., 2013: Mélanges in flysch-type formations: Reviewing geological constraints for a better understanding of complex formations with block-in-matrix fabric, Universita` degli Studi di Napoli Federico II, Dipartimento di Scienze della Terra

Palamakumbura R. et. al., 2012: Geochemical, sedimentary and micropaleontological evidence for a Late Maastrichtian oceanic seamount within the Pindos ocean (Arvi Unit, S Crete, Greece), School of GeoSciences, University of Edinburgh, West Mains Road, Edinburgh, EH9 3JW, UK

Pirazzoli P.A., Thommeret J., Thommeret Y., Laborel J., and Montaggioni L.F., 1982: Tectonophysics 86, 27-43.

Pomoni F., Karakitsios V., 2016: Sedimentary facies analysis of a high-frequency, small-scale, peritidal carbonate sequence in the Lower Jurassic of the Tripolis carbonate unit (central western Crete, Greece): Long-lasting emergence and fossil laminar dolocretes horizons, Department of Geology and Geoenvironment, National and Kapodistrian University of Athens

Rahl J. M. et. al.: Exhumation of high-pressure metamorphic rocks within an active convergent margin, Crete, Greece: A field guide, Jeffrey M. Rahl, Charalampos, Fassoulas, and Mark T. Brandon, Department of Geology and Geophysics, Yale University, New Haven, Connecticut 06511, U.S.A. Natural History Museum of Crete, University of Crete, Heraklion 71409, Greece

Rieger S., 2015: Regional-Scale, Natural Persistent Scatterer Interferometry, Island of Crete (Greece), and Comparison to Vertical Surface Deformation on the Millennial-, and Million-Year Time-Scales; Phd.; Ludwig-Maximilians-Universität München

Seidel M., 2003: Tectono-sedimentary evolution of middle Miocene supra-detachment basins (western Crete, Greece), Ph.D. Dissertation, University of Köln.

Stampfli, 2010: Stampfli Field Course, Tectonostratigraphy and Plate Tectonics of Crete, Université de Lausanne, France

Steiakakis E., 2017: Evaluation of Exploitable Groundwater Reserves in Karst Terrain: A Case Study from Crete; Greece Laboratory of Applied Geology, Technical University of Crete, 73100 Chania, Greece

Thomson S. N. et al., 1989: Apatite fission-track thermochronology of the uppermost tectonic unit of Crete, Implications for the post-Eocene tectonic evolution of the Hellenic Subduction System, Institut für Geologie, Ruhr-Universität Bochum

Thomson S. N., Stockert B., Brix M. R., 1999. Miocene high-pressure metamorphic rocks of Crete, Greece: rapid exhumation by buoyant escape. In: Ring, U., Brandon M. T., Lister G. S., Willetf S. D. (eds): Exhumation Processes: Normal Faulting, Ductile Flow and Erosion. Geological Society, London, Special Publications, 154, 87-107.

Thomson S. N., Stockhert, B. & Brix, M.R. (1998a): Thennochronology of the high-pressure metamorphic rocks of Crete, Greece: implications for the speed of tectonic processes. - Geology 26: 259-262.

Thrust faults: Some common terminology - Geological Digressions https://www.geological-digressions.com

Tiberti M. M., Basili R. & Vannoli P., 2014: Ups and downs in western Crete (Hellenic subduction zone), Istituto Nazionale di Geofisica e Vulcanologia, Via di Vigna Murata 605, 00143 Rome, Italy

Theye, T, Seidel, E. & Vidal, O. (1992): Carpholite, sudoite and chloritoid in low-grade high-pressure metapelites from Crete and the Peloponnese, Greece. - Europ, J. Mineral.4 487-507.

Tortorici L., 2011: The Cretan ophiolite-bearing mélange (Greece): A remnant of Alpine accretionary wedge, Dipartimento di Scienze Geologiche, University of Catania, C.so Italia 55, 95129 Catania, Italy

van Hinsbergen D. J. J., Meulenkamp J. E., 2006: Neogene supradetachment basin development on Crete (Greece) during exhumation of the South Aegean core complex.

Vassilakis E. and Alexopoulos J., 2012: Recognition of Strike-slip Faulting on the Supradetachment Basin of Messara (Central Crete) with remote sensensing Image Interpretation Techniques; National and Kapodistrian University, Department of Dynamics, Tectonics and Applied Geology, Athens, Greece; National and Kapodistrian University, Department of Geophysics & Geothermics, Athens, Greece;

Vandelli A. et. al., 2009: The Lentas unit in Southern Crete: the base of the Pindos sedimentary series? ; Institut de Géologie et de Paléontologie, Université de Lausanne ; New paleontological results Abstract Volume 7th Swiss Geoscience Meeting

Wassmann S., 2012 Geländekurs Kreta

Zachariasse W., van Hinsbergen D., et al. 2011, Formation and Fragmentation of a late Miocene supradetachment basin in central Crete: implications for exhumation mechanisms of high-pressure rocks in the Aegean forearc, Stratigraphy and Paleontology group, Faculty of Geosciences, Utrecht University, Utrecht, The Netherlands; Physics of Geological Processes, University of Oslo

6 Appendix

Geological Time Scale

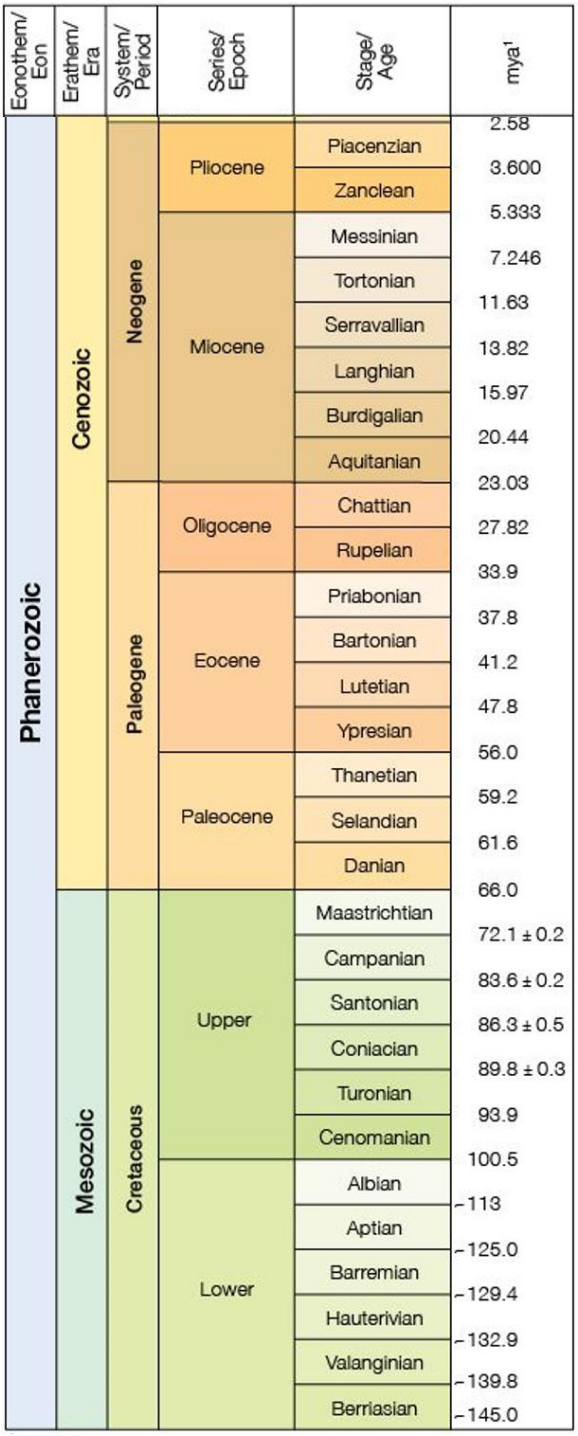

Eonothem/ Eon	Erathem/ Era	System/ Period	Series/ Epoch	Stage/ Age	mya[1]
Phanerozoic	Cenozoic	Neogene	Pliocene	Piacenzian	2.58
				Zanclean	3.600
			Miocene	Messinian	5.333
				Tortonian	7.246
				Serravallian	11.63
				Langhian	13.82
				Burdigalian	15.97
				Aquitanian	20.44
		Paleogene	Oligocene	Chattian	23.03
				Rupelian	27.82
			Eocene	Priabonian	33.9
				Bartonian	37.8
				Lutetian	41.2
				Ypresian	47.8
			Paleocene	Thanetian	56.0
				Selandian	59.2
				Danian	61.6
	Mesozoic	Cretaceous	Upper	Maastrichtian	66.0
				Campanian	72.1 ± 0.2
				Santonian	83.6 ± 0.2
				Coniacian	86.3 ± 0.5
				Turonian	89.8 ± 0.3
				Cenomanian	93.9
			Lower	Albian	100.5
				Aptian	~113
				Barremian	~125.0
				Hauterivian	~129.4
				Valanginian	~132.9
				Berriasian	~139.8
					~145.0

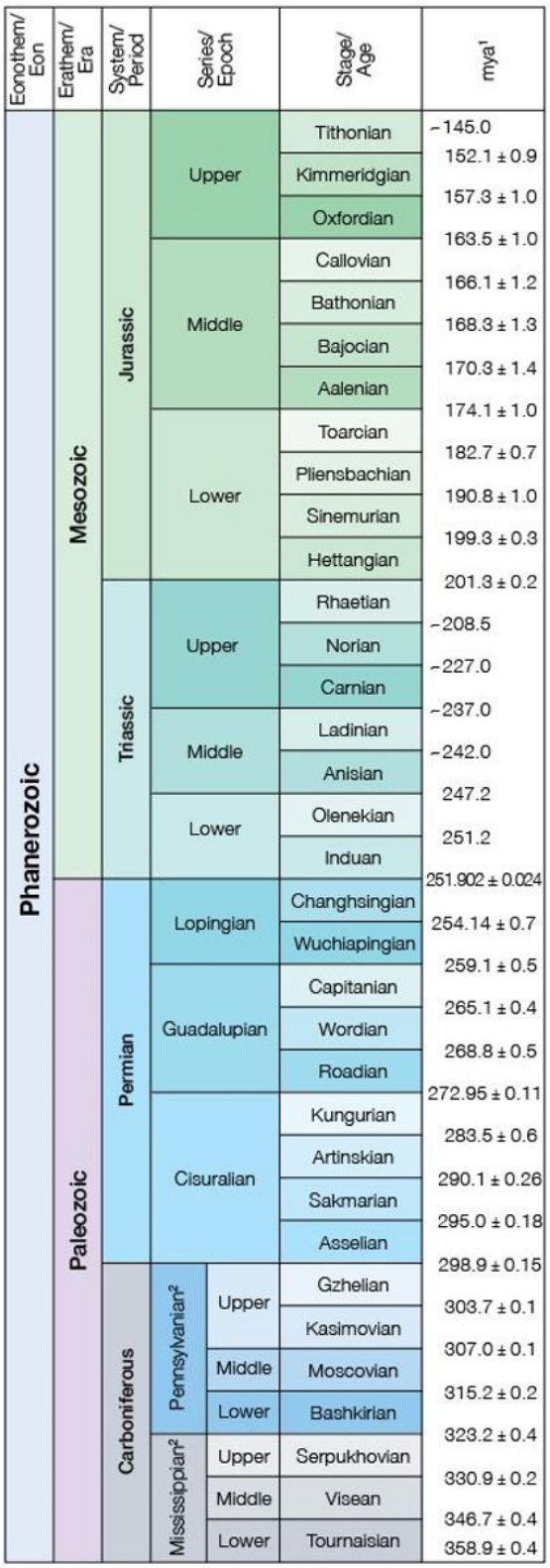

Eonothem/ Eon	Erathem/ Era	System/ Period	Series/ Epoch		Stage/ Age	mya[1]
Phanerozoic	Mesozoic	Jurassic	Upper		Tithonian	~145.0
					Kimmeridgian	152.1 ± 0.9
					Oxfordian	157.3 ± 1.0
			Middle		Callovian	163.5 ± 1.0
					Bathonian	166.1 ± 1.2
					Bajocian	168.3 ± 1.3
					Aalenian	170.3 ± 1.4
			Lower		Toarcian	174.1 ± 1.0
					Pliensbachian	182.7 ± 0.7
					Sinemurian	190.8 ± 1.0
					Hettangian	199.3 ± 0.3
		Triassic	Upper		Rhaetian	201.3 ± 0.2
					Norian	~208.5
					Carnian	~227.0
			Middle		Ladinian	~237.0
					Anisian	~242.0
			Lower		Olenekian	247.2
					Induan	251.2
	Paleozoic	Permian	Lopingian		Changhsingian	251.902 ± 0.024
					Wuchiapingian	254.14 ± 0.7
			Guadalupian		Capitanian	259.1 ± 0.5
					Wordian	265.1 ± 0.4
					Roadian	268.8 ± 0.5
			Cisuralian		Kungurian	272.95 ± 0.11
					Artinskian	283.5 ± 0.6
					Sakmarian	290.1 ± 0.26
					Asselian	295.0 ± 0.18
		Carboniferous	Pennsylvanian[2]	Upper	Gzhelian	298.9 ± 0.15
					Kasimovian	303.7 ± 0.1
				Middle	Moscovian	307.0 ± 0.1
				Lower	Bashkirian	315.2 ± 0.2
			Mississippian[2]	Upper	Serpukhovian	323.2 ± 0.4
				Middle	Visean	330.9 ± 0.2
				Lower	Tournaisian	346.7 ± 0.4
						358.9 ± 0.4

Thrust tectonics - shear zones and accretion wedges

Thrust tectonics

Thrust tectonics or contractional tectonics is concerned with the structures formed by, and the tectonic processes associated with, the shortening and thickening of the crust or lithosphere. It is one of the three main types of tectonic regime, the others being extensional tectonics and strike-slip tectonics. These match the three types of plate boundary, convergent (thrust), divergent (extensional) and transform (strike-slip). There are two main types of thrust tectonics, thin-skinned and thick-skinned, depending on whether or not basement rocks are involved in the deformation. The principle geological environments where thrust tectonics is observed are zones of continental collision, restraining bends on strike-slip faults and as part of detached fault systems on some passive margins.

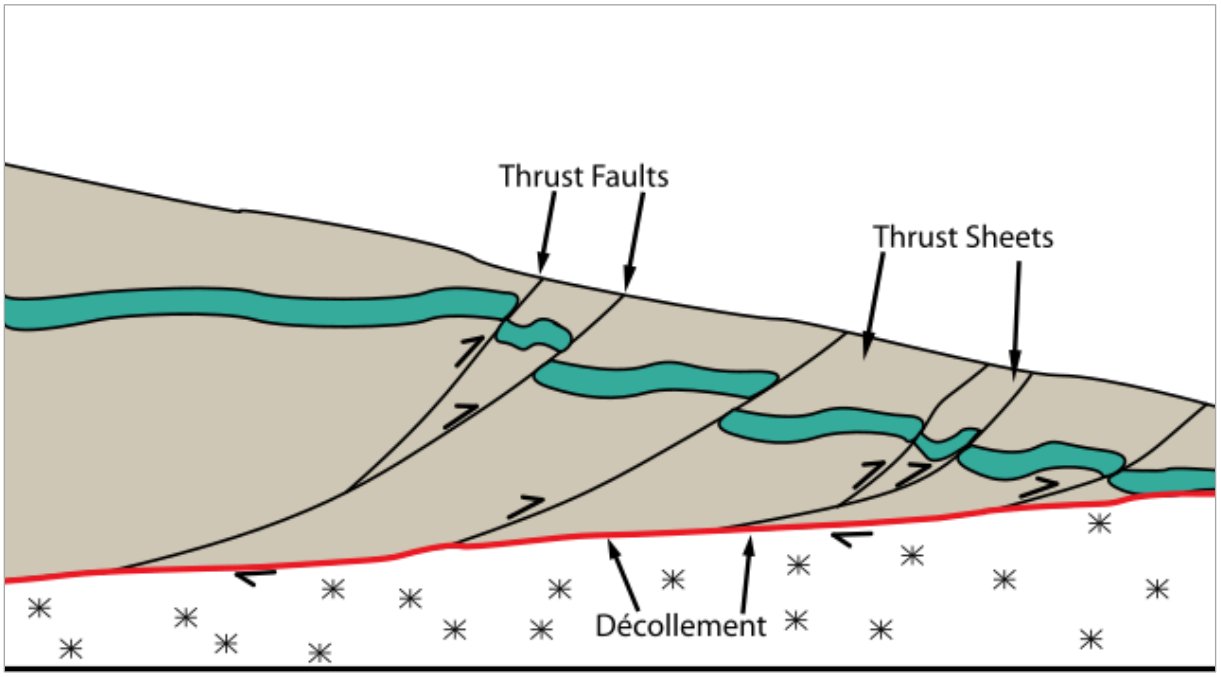

Cross-section diagram of the frontal part of a thin-skinned thrust zone

Deformation styles

In areas of thrust tectonics, two main processes are recognized: thin-skinned deformation and thick-skinned deformation. The distinction is important as attempts to structurally restore the deformation will give very different results depending on the assumed geometry.

Thin-skinned deformation

Thin-skinned deformation refers to shortening that only involves the sedimentary cover. This style is typical of many fold and thrust belts developed in the foreland of a collisional zone. This is particularly the case where a good basal decollement exists such as salt or a zone of high pore fluid pressure.

Thick-skinned deformation

Thick-skinned deformation refers to shortening that involves basement rocks rather than just the overlying cover. This type of geometry is typically found in the hinterland of a collisional zone. This style may also occur in the foreland where no effective decollement surface is present or where pre-existing extensional rift structures may be inverted.

Geological environments associated with thrust tectonics

Collisional zones

The most significant areas of thrust tectonics are associated with destructive plate boundaries leading to the formation of orogenic belts. The two main types are: the collision of two continental tectonic plates (for example the Arabian and Eurasian plates, which formed the Zagros fold and thrust belt) and collisions between a continent and an island arc such as that which formed Taiwan.

Restraining bends on strike-slip faults

When a strike-slip fault is offset along strike such that the resulting bend in the fault hinders easy movement, e.g. a right stepping bend on a sinistral (left-lateral) fault, this will cause local shortening or transpression. Examples include the 'Big Bend' region of the San Andreas fault, and parts of the Dead Sea Transform.

Passive margins

Passive margins are characterised by large prisms of sedimentary material deposited since the original break-up of a continent associated with formation of a new spreading centre. This wedge of material will tend to spread under gravity and, where an effective detachment layer is present such as salt, the extensional faulting that forms at the landward side will be balanced at the front of the wedge by a series of toe-thrusts. Examples include the outboard part of the Niger delta (with an over pressured mudstone detachment) and the Angola margin (with a salt detachment).

Plate Tectonic Model for the Uppermost Nappes of Crete by Tortorici L.

Some parts of the Uppermost Unit bearing ultramafic and mafic rocks embedded in “Wild Flysch” have been referred to as “ophiolitic or Cretan mélange” owing to its complexity and chaotic nature. According to Tortorici L. (2011) the Cretan mélange can be subdivided into three main tectonic units characterized by different metamorphic facies. In Tortorici’s plate tectonic model metamorphism took place during one initial event (so called DA-Event). The three main tectonic units exposed today in South Central Crete each representing a separate nappe are:

1. An un-metamorphosed to weakly metamorphosed lower unit
2. A greenschist to high pressure (HP) greenschist intermediate unit
3. A high pressure/low temperature HP/LT upper unit.

These units display features that associate them with portions of an accretionary wedge [see the Type IV mélange model presented by Cowan (1985)]. In this context, the lower un-metamorphosed to weakly metamorphosed unit is thus interpreted as a tectonic pile built up at the toe of the accretionary wedge where frontal accretion is dominant. In contrast, the metamorphic intermediate and upper units represent the innermost and deeper subducted portions of the accretionary wedge, which were exhumed and superimposed on top of each other during the early stages of continent–continent collision. Owing to the existing tectonic features and metamorphic grade Tortorici, 2011 proposes that the history of the three units can be described by four different continuous compressional events, which he refers to as the DA–DC and DD events.

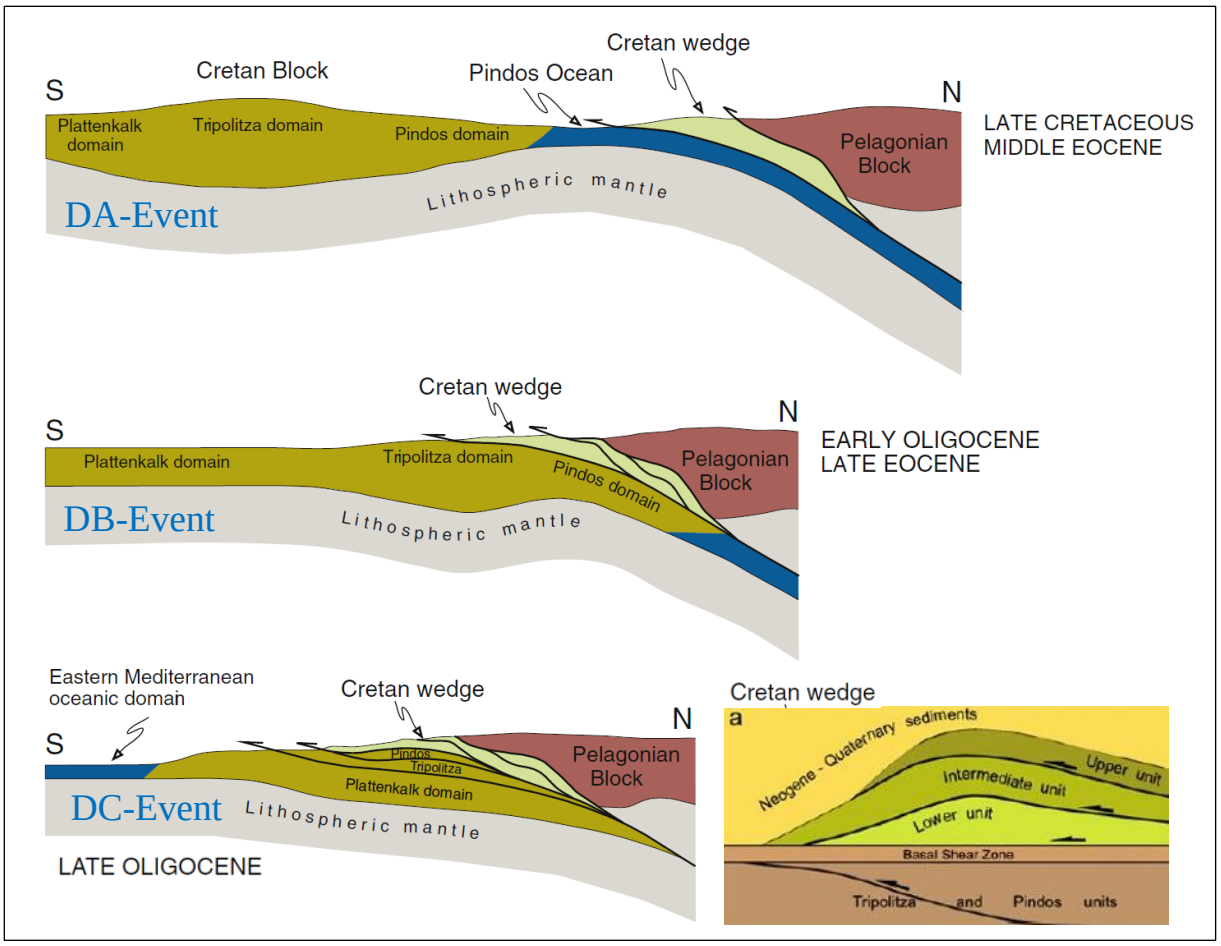

Figure (not to scale) showing the subduction zone between the Pelagonian (Internal Hellenides Platform continental domains) and the Adria (Cretan) blocks. The schematic drawings illustrate the tectonic evolution of the Pindos-Cycladic Ocean (cf. Papanikolaou, 2009) and the Cretan accretionary wedge from the Late Cretaceous to the Late Oligocene. [Tortorici L., 2011]

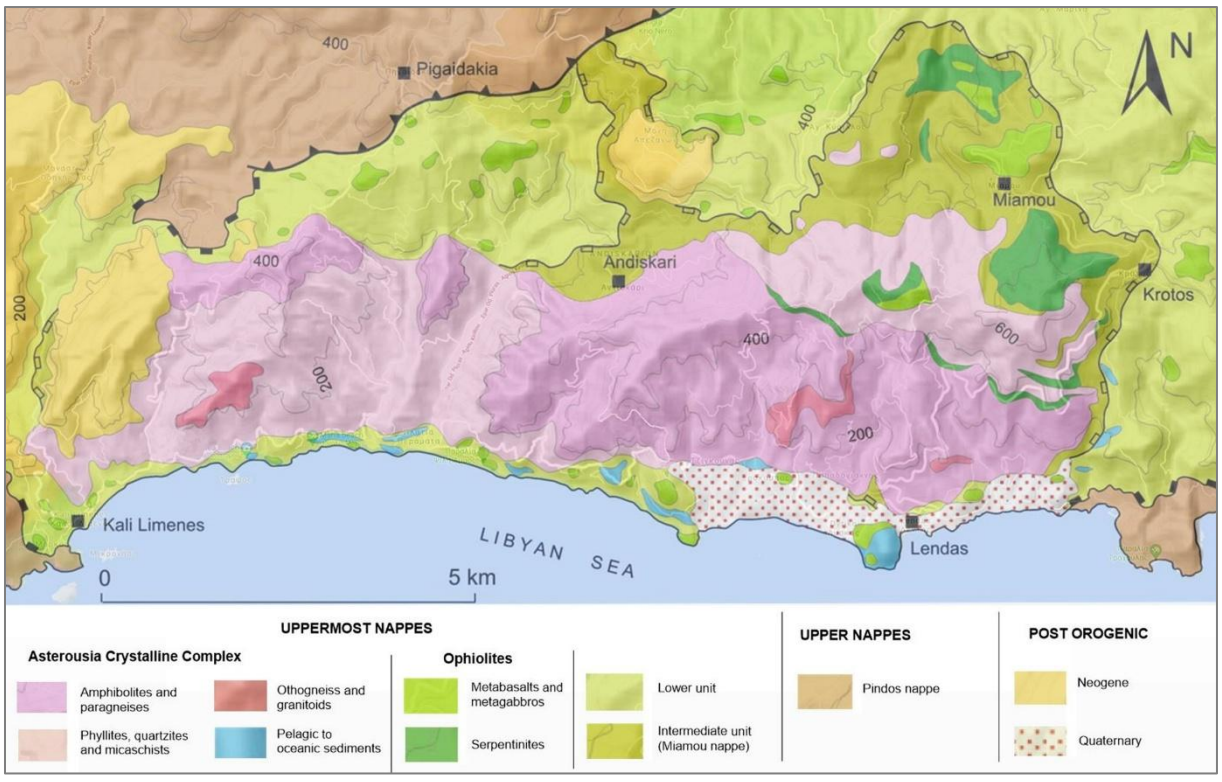

Geological Map of the area Kali Limenes to Lutra showing the division of the Uppermost nappes into subunits based on metamorphic grade (Lower Unit, Intermediate Unit and Asterousia Crystalline Complex; the Upper Unit is not shown on this map as it occurs primarily in the area of Preveli). Modified after Tortorici L. et al., 2011

DA Event

The first DA event produced distinct sets of structures that developed at different crustal levels along major shear zones during oceanic subduction. In the un-metamorphosed lower unit the deformation was mostly related to frontal accretion processes at the toe of the accretionary wedge, while in the intermediate and upper units foliation and metamorphism occurred. The structures and metamorphic features of the intermediate and upper units suggest that these tectono-metamorphic units were exposed to greenschist (P-t values of 7–9 kb and 350 °C) and HP/LT (P-t values of 12–14 kb and 350°–450 °C) overprint during subduction. The Early-Middle Eocene greenschist to blueschist facies metamorphism is thought to be related to the under thrusting of the inner portions of the accretionary wedge beneath the Pelagonian continental basement at a depth of about 35–40 km. At this point the total oceanic lithosphere must have been consumed and the onset of the continental collision was taking place.

DB Event

The primary features of the DA Event were subsequently greatly modified by the DB Event that caused the extrusion and uplift of the two intermediate and upper units along the subduction channel during continental collision. The latest stage of the DB Event produced brittle thrusting of the intermediate and upper units onto the un-metamorphosed portions of the wedge. This caused the reverse stacking of the units and imbrication of ophiolite elements. During the Late Eocene–Early Oligocene the exhumation and emplacement of the intermediate and upper units above the frontal portion of the accretionary wedge was mainly due to deep duplexing (Cello and Mazzoli, 1996; Silver et al., 1985). This involved slices of basement-continental rocks being dragged from the backstop where they were incorporated within the deepest portions of the upper unit. Furthermore, larger blocks such as the Asteroussia continental basement rocks were forced into the shallower portions of the extruded wedge (i.e., the intermediate unit) by thrusting of the overriding plate (Ring and Glodny, 2010).

DC Event

The DC event was dominated by the emplacement of the whole Cretan mélange with its three units onto the continental paleomargin of the Cretan Block (also known as the Adria plate). The entire accretionary wedge was thus incorporated in the continental collision and emplaced in the Late Oligocene–Early Miocene above the Cretan continental margin domains (Tripolitza and Pindos domains). Portions of continental paleodomains (i.e. Plattenkalk and Tripolitza basement) were dragged within the subduction zone and successively stacked and exhumed at the leading edge of the upper plate.

DD Event

Finally, the DD event was characterized by thrusting and folding, which took place during the collision of the two continental margins. This involved the southwestward transport of the entire Cretan nappe pile. From the end of the Early Miocene onwards the headlong continent–continent collision produced a large-scale contractional regime that driven by SSW shortening gave rise to the Cretan segment of the External Hellenides.

Conclusions

Tortorici L. (2011) suggests that the ophiolite bearing units of central Crete represent a suture zone between the southeastern edge of the Adria/Cretan Block to the south, and the Pelagonian continental terranes to the north, which evolved from the closure of the Pindos oceanic domain.

Accretionary prisms and forearc basins at active plate margins

https://www.geological-digressions.com/accretionary-prisms-and-forearc-basins/

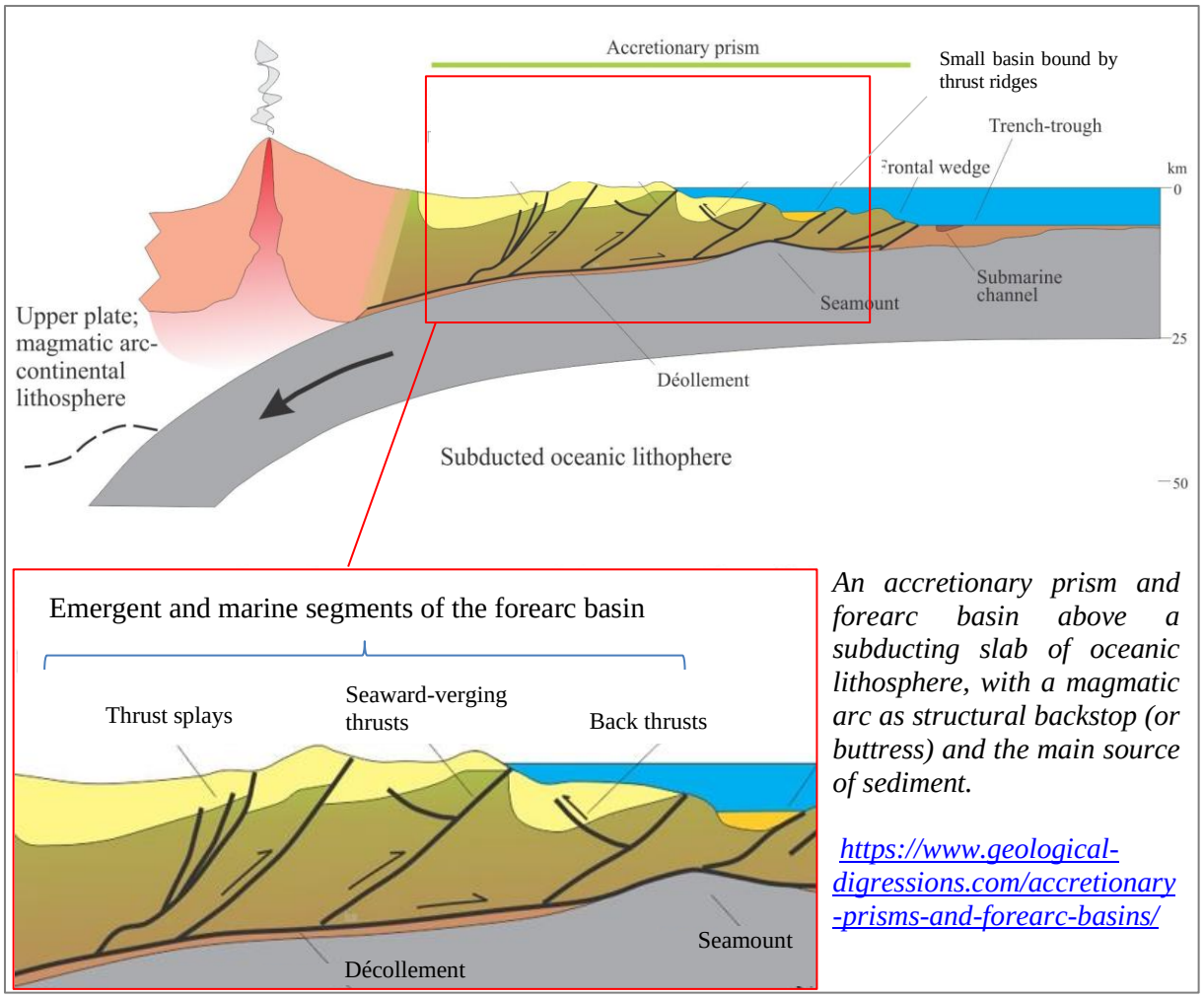

An accretionary prism and forearc basin above a subducting slab of oceanic lithosphere, with a magmatic arc as structural backstop (or buttress) and the main source of sediment.

https://www.geological-digressions.com/accretionary-prisms-and-forearc-basins/

Forearc basins and accretionary prisms are located in the arc-trench gap across accretionary island arc and continent-arc subduction margins. They occupy the upper plate above a descending slab of oceanic lithosphere. As such, they are incredibly dynamic tectono-sedimentary environments; deformation is more or less continuous, driven by large compressive stresses. Sediment sourced from the magmatic arc and related crust is deposited in forearc and trench-slope basins, and in some cases the trench itself. Sediment routing is constantly subjected to modification, in concert with structural changes to sea floor morphology.

The accretionary prism

Accretionary prisms are wedge-shaped stacks of oceanic sediment and some volcanic rock scraped from the top of the subducting lithosphere and plastered over the trench slope. Each slice of sediment is separated by landward-dipping thrusts (i.e. verging towards the trench). Older autochthonous deposits on the upper plate may also be involved in the deformation. Accretion begins at the frontal taper. Landward stacking of thrust panels occurs above a décollement, where the oldest panels are farthest from the trench. The quasi-continuous nature of accretion means that there is jostling along the décollement and the kinematically linked thrust faults through the entire wedge. Like foreland fold-thrust belts, faulting in accretionary prisms is dominated by thrusts**,** fault splays, back-thrusts and out-

of-sequence thrusts. The magnitude of structural shortening across the prism is variable; in some prisms, like that across the Hikurangi margin (New Zealand) a high proportion of shortening is accommodated in the actual subduction zone, rather than in the prism itself (Nicol et al**.** 2007; Open Access).

Prism width can vary considerably along a convergent margin, from a few kilometres to more than 150 km. Wedges thicken up to 20 km landward from the frontal taper.

Thrust panels consist of older autochthonous rocks plus contemporaneous hemipelagic and pelagic sediment (including radiolarian oozes), turbidites and some volcanics. The occasional seamount also gets caught up in the subduction zone causing blockage and major disruption to the wedge front. The intensity of faulting in accretionary prisms results in much penetrative deformation, manifested as fault breccia, boudinage, cleavage, and generally munched up tectonic **mélange**. Mélange can also be derived from slumps, slides, and larger olistostromes, that frequently change the bottom topography on the trench slope.

Late Cretaceous to Early Cenozoic sandstone and mudstone, intensely sheared and incorporated into thrust-related mélange in coastal exposures of the Hikurangi accretionary prism, Waimarama Beach, New Zealand.

The combination of compressional stress, differential deformation, and low sediment permeability results in elevated fluid **pore-pressures** during compaction and faulting. Elevated pore pressures reduce the mechanical (shear) strength of rock and sediment, and thus are partly responsible for the intensity of deformation, particularly in newly accreted thrust slices. Some of this fluid escapes to the sea floor, focused by fault and fracture permeability. Sites of sea floor seepage are identified by their unique cold-water seep faunas, carbonate mounds, and acoustic flares from escaping gas, such as methane (e.g. Barnes et al**,** 2010).

Accretionary prism growth may also take place by **subcretion** in the zone between the wedge and the subducting slab. In this case, thrust slices are added beneath the wedge as duplex-like structures.

There is significant sediment dispersal across the prism, locally filling small basins bound by thrust fault ridges on the trench slope. Sediment routing can change drastically over the life of a prism because of fault-driven changes to sea floor topography. Submarine canyons and gullies also provide pathways for

sediment dispersal across the prism, the lower slope and trench. Sediment transport in this setting is dominated by turbidites and debris flows; submarine slumps and slides also play a significant role on steeper slopes, modifying sediment dispersal routes, and potentially creating loci for dispersal via new gullies.

Sedimentation in the trench

Background sedimentation in the trench (or trough) is primarily pelagic and hemipelagic muds and oozes; if this is the only supply then the trench will be **underfilled**. If sediment bypasses the accretionary prism, the trench may be filled and even **overfilled**. Much of this terrigenous sediment is deposited as sediment gravity flows, where transport is at a high angle to the strike of the trench. However, trench basins are continually under modification because at some stage all this sediment will end up being subducted or incorporated into the accretionary prism.

Axial flow along the trench is also possible via deep submarine channels that are fed by submarine canyons or gullies. In this situation, the axial dispersal of facies will be at a high angle to sediment derived from the accretionary prism. An example of this is located along the Hikurangi subduction margin, where the Hikurangi Channel hugs the margin for more than 800 km.

Critical taper theory

One of the most important kinematic theories used to explain the dynamics of accretionary prisms, is **critical taper theory**. Fold-thrust belts and accretionary prisms are wedge-shaped. In foreland fold-thrust systems the wedge tapers towards the foreland, with the 'push' directed from the hinterland, and where the backstop (that has a buttressing effect) is the craton. In oceanic accretionary prisms, the wedge tapers towards the subducting slab; the rigid backstop is the magmatic arc or some other crustal-scale tectonostratigraphic domain, but in this case the pushing forces are directed towards the prism (and countered by the backstop).

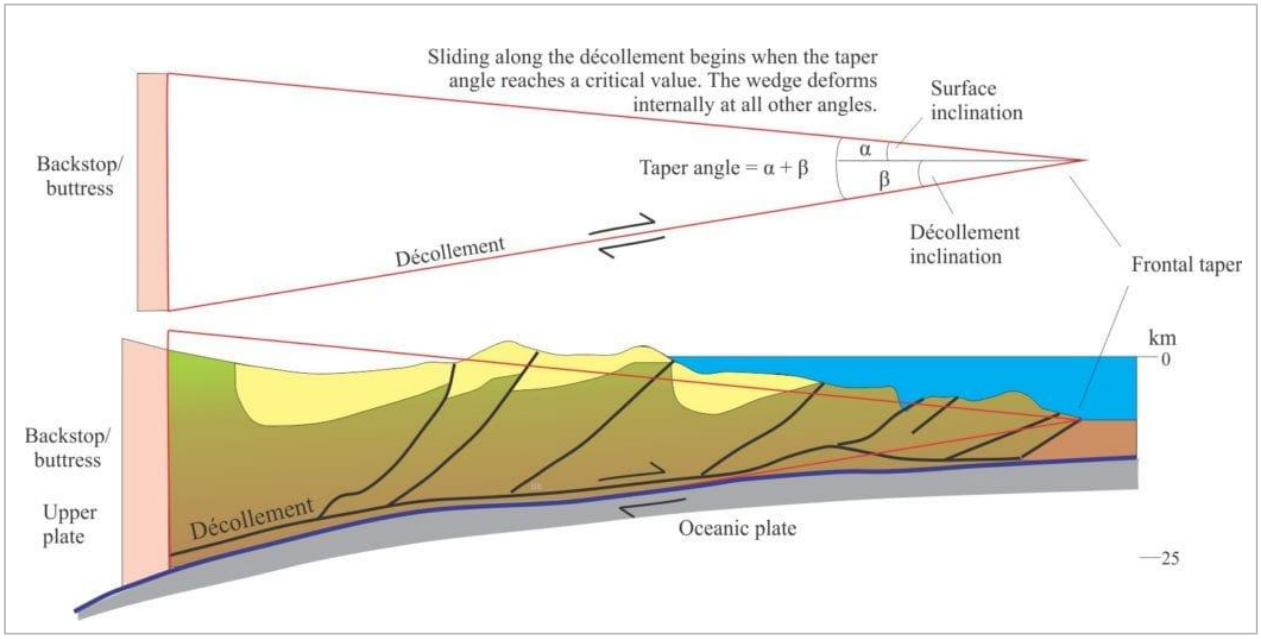

Approximation of an accretionary prism as a wedge, tapered at the subduction-trench boundary. The upper boundary is the prism surface; the lower is the basal décollement. Shear along the décollement will take place when the taper reaches a critical angle.

The analogy of a bulldozer pushing against a pile of snow or sediment illustrates this concept (Davis, Suppe, Dahlem, 1983). As the bulldozer moves forward (applying horizontal compressive stress), the

material accumulates in front of the blade initially as a wedge – at a certain wedge slope the entire mass will begin to slide. Critical taper theory posits that the slope, and therefore the angle of the front taper reaches a critical point depending on the strength of the materials (that may be affected by elevated fluid pressures), the cohesion or frictional forces along the **décollement**, and the slope of that surface. As the critical slope or taper angle is approached, the materials within the wedge will deform – once the critical taper is reached, the entire mass slides along the décollement and there is little subsequent internal deformation of materials other than some minor accommodation along earlier-formed faults (**Chappel**, 1978).

In accretionary prisms, the wedge taper is constantly adjusting to new slices of ocean sediment being structurally added to the front of the wedge, and to sediment deposited across the top of the wedge. This adjustment promotes deformation of the prism along existing thrusts, including the development of out-of-sequence thrusts.

Syn-rift sedimentation at nascent conjugate, passive margins

Nascent conjugate, passive margins - Geological Digressions

Gulf of Aden

Progression of oblique sea floor spreading in Gulf of Aden, although diachronous, has initiated conjugate margins with detectable (on seismic profiles) transitions from continental to oceanic crust. Depth to the Moho decreases from 35 km inland of the Gulf, to about 20 km in the continental-oceanic crust transition.

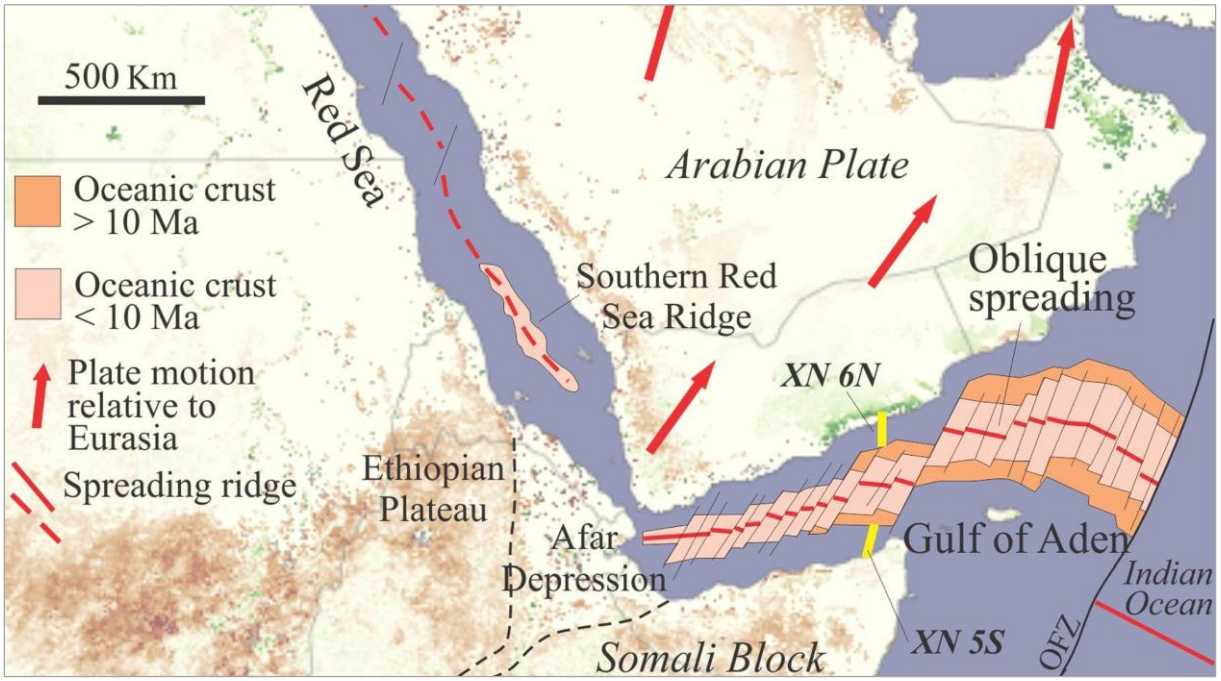

Rift system in the Gulf of Eden indicating the location of Section 6N and 5S shown below

Syn-rift grabens bound by listric faults accommodate coarse-grained clastic, carbonate, and halite-anhydrite deposits 1-2 km thick, and in some troughs >3 km thick. Rotation by syndepositional faulting resulted in numerous stratigraphic discordances.

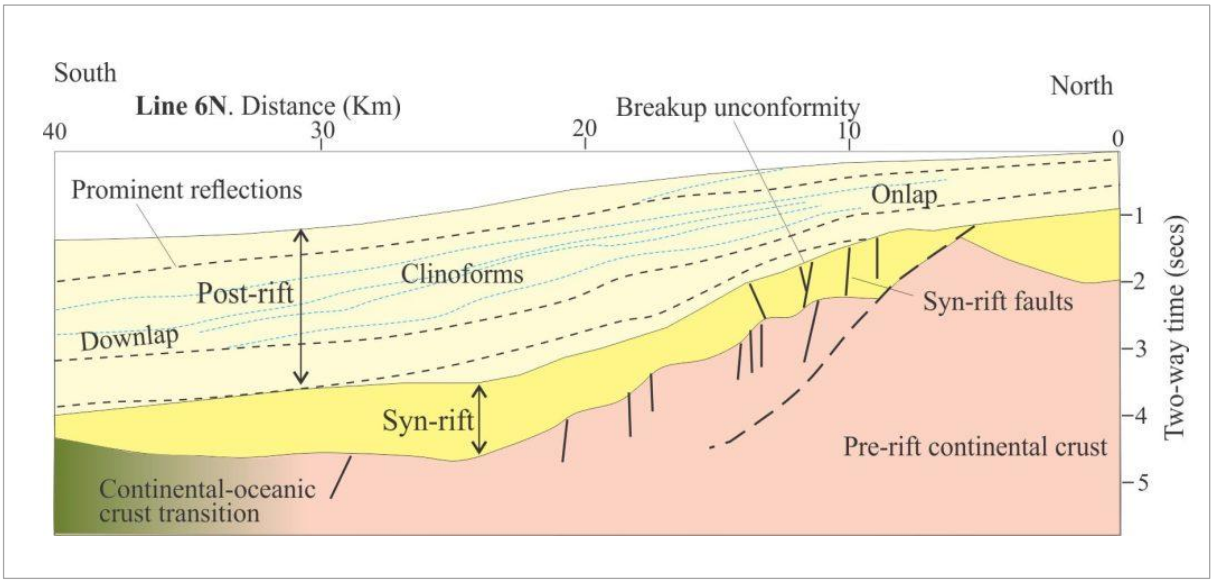

Section 6N, Gulf of Eden

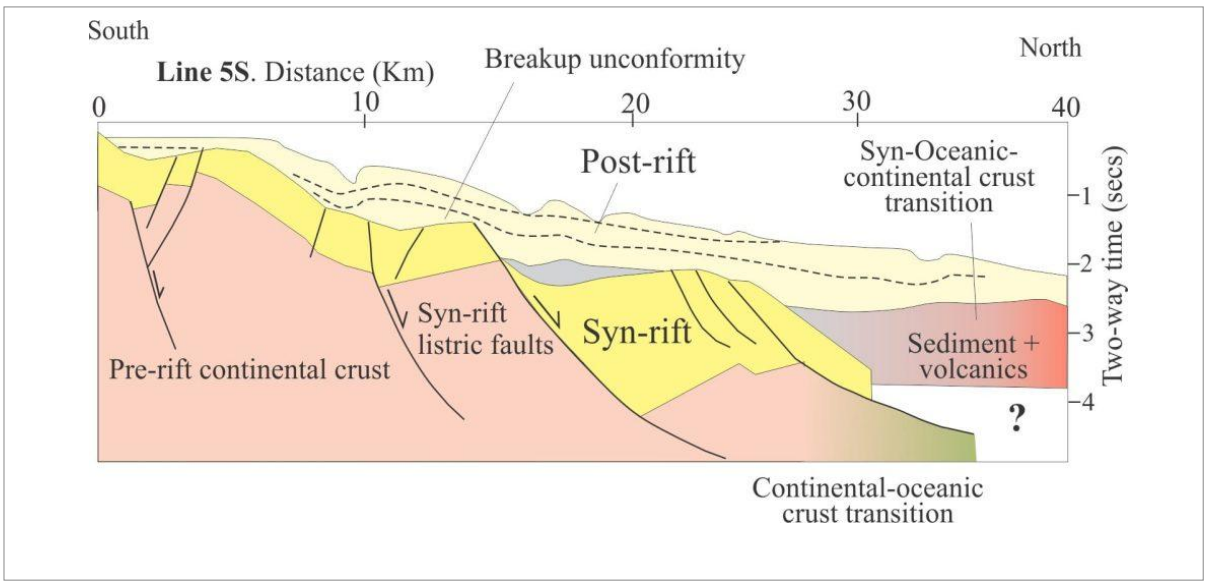

Section 5S, Gulf of Eden

Two profiles across the north (Line 6N) and south (Line 5S) margins of Gulf of Aden interpreted from seismic analysis. Both show the transition from continental crust to crust that is transitional to oceanic. Syn-rift deposits occupy half grabens bound by basin-dipping listric faults, and in turn are unconformably overlain by nascent post-rift, passive margin successions. Prograding clinoforms are well developed in the post-rift succession in Line 6N. Part of the post-rift stage at the basinward end of profile 6N is interpreted as coeval with the continental-oceanic crust transition that probably developed at the beginning of sea floor spreading; the stratigraphic package here includes volcanic accumulations. Modified from Nonn et al. 2019.

Volcanism and intrusion have also played a role in shaping both the syn-rift stage, and the stage where crust transitional between fully continental and fully oceanic formed. In Gulf of Aden, volcanism appears to have been more prominent in the West. The influence of volcanism is apparent in profile 5N where syn-rift and post-rift segmentation of the margin has produced small sub-basins and stratigraphic on lap of associated depositional packages.

The overlying paired passive margin successions extend from a depositional edge near the modern coast, to 2-3 km thick offshore. Some seismic profiles show well defined clinoforms with shoreward onlap and basinward downlap geometries. A mid-Miocene unconformity between the syn-rift and post-rift (drift) sedimentary packages is interpreted as a break-up unconformity. Note that this unconformity is older than that in the Red Sea region (end of Miocene). (*At Geological Digressions there is a companion post that looks at the initiation of continental rifting in the East African Rift System (EARS) and a couple of early but relevant models of rift to passive margin transitions).*

Types of Mid-Ocean Ridge Basalts (MORB)

N-MORB stands for Normal Mid-Ocean Ridge Basalt**,** which is a type of basalt found at mid-ocean ridges. It is characterized by its depletion in incompatible elements, meaning it has lower concentrations of elements like potassium, rubidium, and barium compared to other basalt types. This depletion occurs because N-MORB originates from a mantle source that has undergone previous melting events, removing these elements.

Mid-Ocean Ridge Basalts are classified based on their geochemical composition and mantle source characteristics. The main types include:

N-MORB (Normal MORB) – As mentioned, this type is depleted in incompatible elements and represents the typical basalt found at mid-ocean ridges.

E-MORB (Enriched MORB) – Contains higher concentrations of incompatible elements, suggesting it originates from a mantle source that has been enriched by previous melt interactions.

T-MORB (Transitional MORB) – Falls between N-MORB and E-MORB in terms of composition, showing moderate enrichment in incompatible elements.

BABB (Back-Arc Basin Basalt) – Found in back-arc basins near subduction zones, these basalts have compositions influenced by subduction-related processes.

MORB plays a crucial role in understanding mantle dynamics and plate tectonics, as it provides insights into the composition and evolution of Earth's mantle.